

Poisson Distribution based algorithm to reduce grid harmonics caused by EV chargers

by

Yadunath Sapkota

A thesis submitted to the

School of Graduate and Postdoctoral Studies in partial

fulfillment of the requirements for the degree of

Master of Science in Electrical and Computer Engineering

ECE Department/Ontario Tech University/ Dr. Vijay K. Sood

University of Ontario Institute of Technology (Ontario Tech University)

Oshawa, Ontario, Canada

December 2023

© Yadunath Sapkota, 2023

THESIS EXAMINATION INFORMATION

Submitted by: **Yadunath Sapkota**

Master of Science in Electrical and Computer Engineering

Thesis title: Poisson Distribution based algorithm to reduce grid harmonics caused by EV chargers.
--

An oral defense of this thesis took place on December 12, 2023 in front of the following examining committee:

Examining Committee:

Chair of Examining Committee	Dr. T. Sidhu
Research Supervisor	Dr. Vijay K. Sood
Examining Committee Member	Dr. S. Williamson
Thesis Examiner	Dr. B. Reddy

The above committee determined that the thesis is acceptable in form and content and that a satisfactory knowledge of the field covered by the thesis was demonstrated by the candidate during an oral examination. A signed copy of the Certificate of Approval is available from the School of Graduate and Postdoctoral Studies.

ABSTRACT

The global market of electric vehicles (EVs) is growing rapidly because of several factors such as growing concerns for pollution, governmental incentives/subsidies and regulations and consumers' increasing interest in quiet, pollution-free vehicles. Many countries are determined to sell only EVs from 2035 onwards. With the increase of EVs, fast charging stations need to be installed at many facilities such as universities, shopping malls, hospitals, parking facilities etc. When many EVs start plugging into these facilities to charge, the grid power quality is expected to deteriorate, so it is important that the grid power quality be maintained in the most economical way possible.

In this thesis, a new statistics-based algorithm is proposed to reduce the grid harmonics caused by EVs which are essentially non-linear loads. The proposed algorithm helps reduce grid harmonics by phase-shifting the carrier waves of each charging bay within a charging station. When the carrier waves are phase-shifted, the switching transients are distributed over time and some of the generated harmonics will cancel each other. This technique does not require any centralized communication or information exchange between the charging bays to coordinate the carrier waves. As an example, the algorithm is implemented in twenty (20) bays within a charging station by utilizing the Mean and Variance values of the Cumulative Poisson Distribution. This methodology is implemented using MATLAB Simulink platform and the performance is validated. The techniques have demonstrated a 30% improvement in the power quality of the grid voltage.

Keywords: Electric Vehicles (EVs); Electric grid; Power quality; harmonics; Poisson Distribution

AUTHOR'S DECLARATION

I hereby declare that this thesis consists of the original work of which I have authored. This is a true copy of the thesis, including any required final revisions, as accepted by my examiners.

I authorize the University of Ontario Institute of Technology (Ontario Tech University) to lend this thesis to other institutions or individuals for the purpose of scholarly research. I further authorize University of Ontario Institute of Technology (Ontario Tech University) to reproduce this thesis by photocopying or by other means, in total or in part, at the request of other institutions or individuals for the purpose of scholarly research. I understand that my thesis will be made electronically available to the public.

Yadunath Sapkota

YADUNATH SAPKOTA

STATEMENT OF CONTRIBUTIONS

Part of the work described in the thesis has been published as:

A. Conference Paper:

1. **Y. Sapkota**, A. Shier, V.K. Sood, “Statistics-Based Algorithm to Reduce Grid Harmonics due to EV Chargers”, 5th International Conference on Energy, Power, and Environment (ICEPE 2023) TOWARDS FLEXIBLE GREEN ENERGY TECHNOLOGIES, Conference National Institute of Technology Meghalaya, India. 15th-17th June 2023.

ACKNOWLEDGEMENTS

I would like to express my gratitude and sincere thanks to my supervisor Dr. Vijay K. Sood, for his valuable guidance, suggestions, inspiration, and support throughout this research work.

I would also like to express my special thanks to Ahmed Sheir for his very valuable advice and support.

TABLE OF CONTENTS

ABSTRACT	iii
AUTHOR’S DECLARATION.....	iv
STATEMENT OF CONTRIBUTIONS	v
ACKNOWLEDGEMENTS.....	vi
LIST OF FIGURES	ix
LIST OF ABBREVIATIONS AND SYMBOLS	xi
Chapter 1. Introduction.....	1
1.1 Context	1
1.1.1 Electrical vehicles (EVs) in Canada and the world trend	1
1.1.2 Types of EVs.....	3
1.1.3 Types of charging levels	4
1.2 Impacts of EV chargers on power grid.....	6
1.3 Power Quality Standards	7
1.4 Problem Formulation.....	10
Chapter 2. Literature review	13
2.1 Literature review	13
2.2 Motivation	18
Chapter 3. The Proposed Approach.....	20
3.1 The proposed algorithm.....	20
3.2 Utilization of Poisson Distribution.....	21
3.2.1 Poisson Distribution.....	21
3.2.2 Cumulative Poisson Distribution	22
3.2.3 Inverse Poisson Distribution	23
3.3 Carrier wave phase shift calculation using Poisson Distribution	24
3.4 Discussion, Results and Simulation	30
Chapter 4. System Description	35
Chapter 5. Conclusions.....	38
5.1 Conclusion Summary	38
5.2 Future scope	39
REFERENCES	41
APPENDICES	49

LIST OF TABLES

Table 1. 1: Types of Charging levels.....	5
Table 1. 2: IEEE Standard 519-2014: Voltage distortion limits.....	9
Table 1. 3: IEEE Standard 519-2014: Current distortion limits (120 V to 69 kV)	9
Table 1. 4: IEEE Standard 519-2014: Current distortion limits (69 kV to 161 kV)	9
Table 1. 5: IEEE Standard 519-2014: Current distortion limits (above 161 kV).....	10
Table 3. 1: Phase shifts calculation for $\lambda = 15$	29
Table 3. 2: THD results summary.....	34

LIST OF FIGURES

Figure 1. 1: Global electric passenger car stock, 2010-2020, appears in Global EV Outlook 2021	2
Figure 1. 2: Flow chart showing 3 levels of charging	4
Figure 1. 3: Ideal phase shift when (a) two chargers (b) four chargers or (c) eight chargers operating in parallel	12
Figure 3. 1: Carrier wave phase shift calculation algorithm.....	25
Figure 3. 2: Cumulative Poisson Distribution for $\lambda = 5, 10$ and 15	27
Figure 3. 3: Triangular carrier waveforms showing the calculated phase-shift for 6 selected cases (shaded rows) from Table 3.1	28
Figure 3. 4: Harmonic profiles and harmonic distortion in grid voltage and grid current	32
Figure 3. 5: Benchmark harmonic profiles and harmonic distortion in grid voltage and current	32
Figure 3. 6: Results summary for grid voltage	34
Figure 3. 7: Results summary for grid current.....	35
Figure 4. 1: System representation	35
Figure 4. 2: Simulink model of the system with 20 bays	36
Figure 4. 3: Control mechanism of a charging bay consisting of carrier phase shift algorithm, VSC control and DC-DC converter	37
Figure A. 1: Bernoulli Distribution with equal probability	49
Figure A. 2: Bernoulli Distribution with unequal probability	50
Figure B. 1: Bernoulli and Binomial Distributions	51
Figure B. 2: Binomial distribution when probability of success and failure are equal	52

Figure B. 3: Binomial distribution when the probability of success and failure are not equal 53

Figure D. 1: Normal distribution curves constant Variance and varying Mean..... 56

Figure D. 2: Graphs showing the shifting of the plots to the right as the Mean value increases 57

Figure D. 3: Normal distribution curves with constant Mean and varying Variance values.. 58

Figure D. 4: Graphs showing the steepness of the curves as the variance decreases 59

Figure E. 1: Bar graphs showing the behavior of the Poisson Distribution as the Mean value varies..... 63

Figure E. 2: Behavior of the Cumulative Poisson Distribution as the Mean value varies 64

LIST OF ABBREVIATIONS AND SYMBOLS

EVs	Electric Vehicles
BEVs	Battery Electric Vehicles
HEVs	Hybrid Electric Vehicles
PHEVs	Plug-in Hybrid Electric Vehicles
IEA	International Energy Agency
GHG	Greenhouse Gas
THD	Total Harmonic Distortion
EMC	Electromagnetic Compatibility
SAE	Society of Automotive Engineers
ANSI	American National Standard Institute
IEC	International Electrotechnical Commission
PCC	Point of Common Coupling
FCS	Fast Charging Stations
ANN	Artificial Neural Network
IIR	Infinite Impulse Response
SVM	Space Vector Modulation
D-STATCOM	Distribution Static Synchronous Compensator
CF	Confidence Factor
GN	Guessed Number
VSC	Voltage Source Converter
F_c	Triangular Carrier Wave Frequency
PMF	Probability Mass Function

Chapter 1. Introduction

1.1 Context

1.1.1 Electrical vehicles (EVs) in Canada and the world trend

The global market for EVs continues to increase rapidly due to the growing concerns over greenhouse gas (GHG) emissions, the tighter emission regulations, improvement in affordability and reliability of batteries, and government incentives for EVs etc. Governments around the world are setting goals to switch from gasoline cars to EVs within almost a decade. Canada is banning the sale of new fuel-powered cars and light trucks from 2035. Similarly, Norway, Belgium, and Austria are banning gas powered cars from 2025, 2026, 2027, respectively. Also, Germany, Iceland, India, and some other countries are banning them from 2030 onwards. As the governments have set goals, so have the car companies. Honda has aimed to electrify two-thirds of its global automobile sales by 2030. BMW expects at least half of its sales to be electric cars by 2030 onwards, and Ford is committed to become carbon neutral by 2050. Similarly, almost all the car companies will comply with the governments' rules worldwide. Clearly, the world is moving rapidly towards EVs. Tesla is a leading EV manufacturer based in California, United States which is gaining popularity. BMW has already launched all-electric models BMW iX, BMW i3 and BMW i3s which are advertised as both "emission-free and silently gliding cars"! Similarly, Toyota has launched the Prius Prime and RAV4 Prime as plug-in hybrids. All the other main car companies have also come up with some models that are purely electric or hybrid cars. The government of Canada has also given good incentives for its residents to use EVs. The incentives range from \$625 to \$5000 depending on the make and model of the cars. The USA also provides federal income tax credits of up to \$7500 for EVs.

The Journal of Commerce says that “In 2020, global sales of EVs, made up of battery electric vehicles (BEVs) and plug-in hybrid electric vehicles (PHEVs), increased by +43% to 3.2 million units”. The main factor for the emergence of EVs is environmental. Recently, G7 countries have announced that zero-emission vehicles should replace the gas vehicles.

According to International Energy Agency (IEA), as shown in Figure 1.1, “more than 10 million electric cars were on the world’s roads in 2020 with battery electric models driving the expansion” [1].

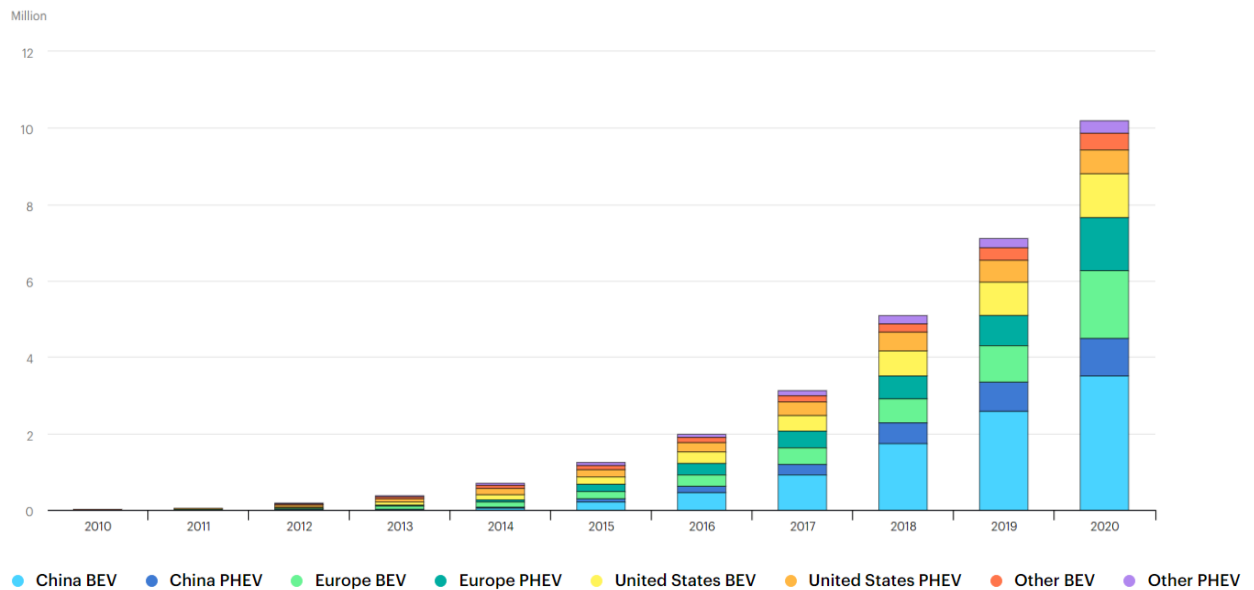


Figure 1. 1: Global electric passenger car stock, 2010-2020, appears in Global EV Outlook 2021

According to the Government of Canada, the transportation sector is responsible for 27 percent of greenhouse gas (GHG) emissions in Canada. Light-duty vehicles—the cars, vans and light-duty trucks are responsible for almost half of that total. Similarly, The Globe and Mail maintains that the light-duty vehicles and light-duty trucks account for nearly half of all GHG emissions from the transportation category which is 35 percent in the US. According to Statistics Canada, there were 1542561 light vehicles registered in Canada in 2020 of which

only 95806 were Battery, Hybrid, and Plug-in Hybrid Electric Vehicles (PHEVs). Similarly, there were 275 million vehicles registered in the US in the same year, according to CEIC data. So, it is obvious that the number of vehicles will keep increasing in the decades to come, and most of them will be EVs.

1.1.2 Types of EVs

There are three types of EVs available: Battery-powered electric vehicles (BEVs), hybrid electric vehicles (HEVs) and plug-in hybrid electric vehicles (PHEVs).

- Battery electric vehicles are powered solely by electric batteries and are propelled by electric motors. BEVs are fully electric vehicles, they use no gasoline, and all energy comes from the battery pack which is recharged from the grid.
- Hybrid electric vehicles have both an internal combustion engine and one or more electric motors to drive the vehicle. The battery is not charged by connecting it to the power grid, rather it receives all its energy from regenerative braking, which recoups otherwise lost energy in braking to assist the gasoline engine during acceleration. In a traditional internal combustion engine vehicle, this braking energy is normally lost as heat in the brake pads and rotors.
- Like regular hybrid vehicles, plug-in hybrid electric vehicles also have both an internal combustion engine and an electric motor to drive the vehicle. Unlike in regular hybrid, the battery in PHEV is much larger and can be recharged both by plugging into the grid and by regenerative braking. Once the battery is discharged, PHEVs run in hybrid mode and can travel a longer distance with less gas compared to purely gasoline cars since they still have two sources of power: gasoline and battery powered by regenerative braking.

1.1.3 Types of charging levels

There are two main types of EV chargers: AC chargers and DC chargers. As shown in Figure 1.2, AC chargers have two levels of charging: Level 1 and Level 2. The DC chargers are Level 3 charging. The AC chargers provide alternating current electricity to the vehicles and each vehicle's on-board converter converts the AC to DC. However, DC chargers, also known as fast chargers, provide direct current electricity to the vehicle.

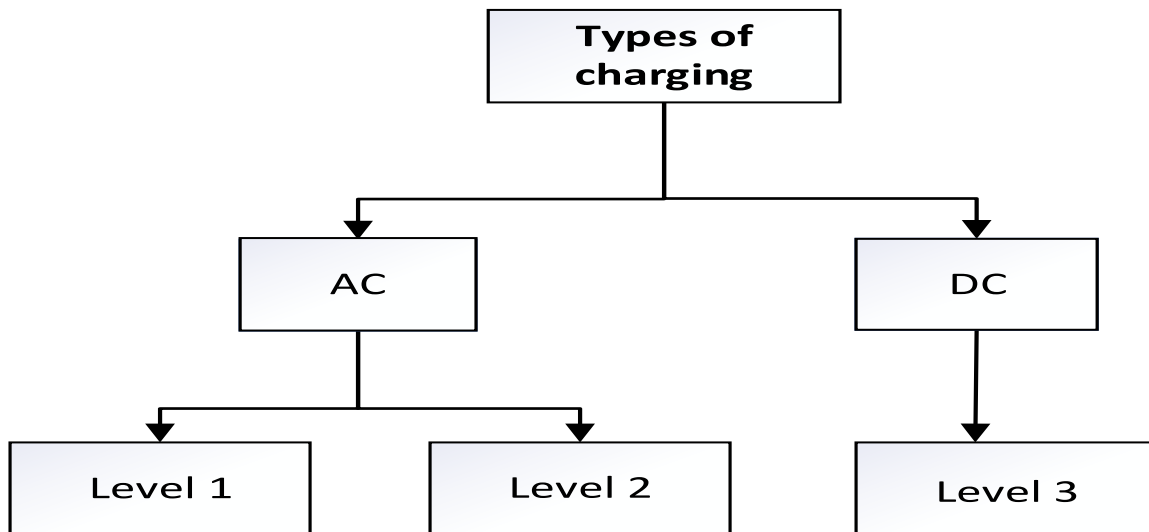





Figure 1. 2: Flow chart showing 3 levels of charging.

- Level 1 charging is very slow charging and can be used at home with the regular power outlet of 110-120 V. It takes 12 to 24 hours to fully charge a battery. Since it is very slow and it trickles electricity into the battery, it is also known as trickle charging.
- Level 2 charging is much faster than Level 1 charging. It uses a 240 V outlet, like what is used for a dryer. This charger can charge a car in 2 to 4 hours.
- Level 3 chargers are also called DC fast chargers. This charger can charge a car in 20 to 40 minutes. Since these chargers are expensive, these chargers are practically

feasible only for public locations. Table 1.1 shows the classification of the three levels of charging [2-4].

Table 1. 1: Types of charging levels

Charger Description	Level 1	Level 2	Level 3
Type	Standard wall outlet (AC)	Charging Station (AC)	DC Fast charging
AC to DC converter	On-board	On-board	Off-board
Charging Speed	Slow	Mid-range	Fast
Typical charging time	12 hours for a completely discharged 16-kWh battery	3 hours for a completely discharged 16-kWh battery	80% in 20 min.
Voltage	120 V	208 or 240 V	200 to 450 V
Power	1.4 kW	7.2 kW	50 kW
Equipment	 <p>Source: NEMA</p>	 <p>Source: NEMA</p>	 <p>Source: LEVITON</p>

1.2 Impacts of EV chargers on power grid

As the world prepares for net zero-emission vehicles within the next two decades, EVs will come with both opportunities and challenges since they will create millions of jobs as the world goes green. The most challenging part of EVs is the charging factor: the infrastructures needed for charging batteries, and efficient and inexpensive rechargeable batteries. The infrastructure includes grid capacity, grid power quality, charging stations, charging behavior etc. The existing grid infrastructure may not be sufficient for many EVs to plug in and charge all at the same time. Even when the infrastructures are enhanced, if many cars are plugged in at the same time, they will impact the power quality injecting harmonics into the grid. The focus of this research is on grid power quality.

Within the grid, primarily the impacts of EV chargers will be felt on the transformers and transmission lines. As a result, transformers will age sooner affecting their life span. Not only will the transformers suffer from extra heating, but so will the transmission lines. The impacts of EV chargers on the distribution transformer are discussed in [5]. It concludes that as large numbers of EVs are charged at the same time, the distribution transformer will be facing an extra load, which increases the aging accelerating factor (F_{AA}) which can shorten the life of the transformers. Similarly, [6] presents the effects like voltage deviation, voltage imbalance between the 3-phases and sequence components. It compares the imbalance in line-to-neutral, line-to-line, negative sequence and zero sequence voltages. The impact of plug-in-vehicles on distribution networks in large scale distribution planning model is presented in [7].

Overvoltage and undervoltage are other impacts caused by EVs. Electric surges are the results of sudden releases of energy that was previously stored in the batteries. Repeat transients are frequently caused by the switching of reactive circuit components such as

inductors and capacitors. Undervoltage is caused by EVs when many vehicles are connected to the grid at the same time. The undervoltage is dependent on the charging characteristics, time of charging and penetration level.

One of the most alarming impacts of EV chargers is the increase of Total Harmonic Distortions (THDs) in the grid voltage. The presence of harmonics in the power grid is an increasing concern as the penetration of EVs is increasing. Since many power-electronic elements are used to convert the grid AC to DC power needed to charge the batteries, the EV chargers cause harmonics. The harmonic pollution depends directly on the number of EVs and the charging methods. The harmonics not only have damaging effects on the equipment connected to the network, but they can also cause malfunctions to the protection system.

EV chargers can also create fast voltage fluctuations, which may cause flickering problems. The magnitude of fluctuations depends on the transient charging peak current and impedance of the grid.

1.3 Power Quality Standards

Since EV loads vary based on the levels of charging and types of batteries, the adverse impacts they can have on the grid power quality need to be addressed properly. Different organizations such as the Institute of Electrical and Electronics Engineers (IEEE), the Society of Automotive Engineers (SAE), the International Electrotechnical Commission (IEC), American National Standard Institute (ANSI), etc. have produced standards to determine the power quality impacts and to maintain the power quality. The following is the list of some of the relevant standards produced by the afore mentioned organizations.

- IEEE Std 519-2014: IEEE Recommended Practices and Requirements for Harmonic Control in Electrical Power Systems
- IEEE Std 1159-2019: IEEE Recommended Practice for Monitoring Electric Power Quality
- IEEE Std 1453-2015: IEEE Recommended Practice: Adoption of IEC 61000-4-15:2010, Electromagnetic compatibility (EMC)—Testing and measurement techniques—Flicker meter—Functional and design specifications.
- IEEE Std 1564-2014: IEEE Guide for Voltage Sag Indices
- IEC Standard 61000-3-2, Electromagnetic compatibility (EMC)-Limits for harmonic current emission (equipment input current ≤ 16 A per phase)
- IEC 61000-3-3, Electromagnetic compatibility (EMC)—Limitation of voltage changes, voltage fluctuations and flicker in public low-voltage supply systems for equipment
- IEC 61000-3-4, Electromagnetic compatibility (EMC)—Limitation of emission of harmonic currents in low-voltage power supply systems for equipment with rated current greater than 16A.
- IEC 61000-3-12, electromagnetic compatibility (EMC)—Limits for harmonic currents produced by equipment connected to public low-voltage systems with input current >16 A and ≤ 75 A per phase.
- SAE standard J2894/1_201901 defines power quality requirements for Plug-in Electric Vehicle Chargers.

Similarly, IEEE standard 519-2022 compliance criteria suggests the limits for voltage and current distortions which are listed in Tables 1.2-1.4 [8].

Table 1. 2: IEEE Standard 519-2022: Voltage distortion limits

Voltage distortion limits		
Bus voltage at PCC	Individual harmonic (%) $h \leq 50$	Total harmonic distortion THD (%)
$V \leq 1.0$ kV	5.0	8.0
$1\text{kV} < V \leq 69\text{kV}$	3.0	5.0
$69\text{kV} < V \leq 161\text{kV}$	1.5	2.5
$V > 161\text{kV}$	1.0	1.5*

*High-voltage systems are allowed to have up to 2.0% THD where the cause is an HVDC terminal whose effects are found to be attenuated at points in the network where future users may be connected.

Table 1. 3: IEEE Standard 519-2022: Current distortion limits (120V to 69kV)

Current distortion limits rated 120 V – 69 kV (Individual harmonic order^b)						
I_{SC}/I_L	$2 \leq h < 11^a$	$11 \leq h < 17$	$17 \leq h < 23$	$23 \leq h < 35$	$35 \leq h < 50$	TDD
$<20^c$	4.0	2.0	1.5	0.6	0.3	5.0
20 to < 50	7.0	3.5	2.5	1.0	0.5	8.0
50 to <100	10.0	4.5	4.0	1.5	0.7	12.0
100 to < 1000	12.0	5.5	5.0	2.0	1.0	15.0
>1000	15.0	7.0	6.0	2.5	1.4	20.0

where,

I_{SC} = maximum short-circuit current at PCC

I_L = maximum demand load current at PCC under normal load operating conditions

^a For $h \leq 6$, even harmonics are limited to 50% of the harmonic limits

^b Current distortions that result in a dc offset, e.g., half-wave converters, are not allowed

^c Power generation facilities are limited to these values of current distortion, regardless of actual I_{SC}/I_L unless covered by other standards with applicable scope.

Table 1. 4: IEEE Standard 519-2022: Current distortion limits (69 kV to 161 kV)

Current distortion limits rated 69 V – 161 kV (Individual harmonic order^b)						
I_{SC}/I_L	$2 \leq h < 11^a$	$11 \leq h < 17$	$17 \leq h < 23$	$23 \leq h < 35$	$35 \leq h < 50$	TDD
$<20^c$	2.0	1.0	0.75	0.3	0.15	2.5
20 to < 50	3.5	1.75	1.25	0.5	0.25	4
50 to <100	5.0	2.25	2.0	0.75	0.35	6.0
100 to < 1000	6.0	2.75	2.5	1.0	0.5	7.5
>1000	7.5	3.5	3.0	1.25	0.7	10.0

^a For $h \leq 6$, even harmonics are limited to 50% of the harmonic limits

^b Current distortions that result in a dc offset, e.g., half-wave converters, are not allowed

^c Power generation facilities are limited to these values of current distortion, regardless of actual I_{SC}/I_L unless covered by other standards with applicable scope.

Table 1. 5: IEEE Standard 519-2022: Current distortion limits (above 161 kV)

Current distortion limits rated > 161kV (Individual harmonic order^b)						
I_{SC}/I_L	$2 \leq h < 11^a$	$11 \leq h < 17$	$17 \leq h < 23$	$23 \leq h < 35$	$35 \leq h < 50$	TDD
$< 20^c$	1.0	0.5	0.38	0.15	0.1	1.5
20 to < 50	2.0	1.0	0.75	0.3	0.15	2.5
≥ 50	3.0	1.5	1.15	0.45	0.22	3.75

^a For $h \leq 6$, even harmonics are limited to 50% of the harmonic limits

^b Current distortions that result in a dc offset, e.g., half-wave converters, are not allowed

^c Power generation facilities are limited to these values of current distortion, regardless of actual I_{SC}/I_L unless covered by other standards with applicable scope.

1.4 Problem Formulation

Numerous ways exist for reducing harmonics generated by converters operating in parallel. One way is to interleave their operation. Converters use triangular carrier-waves to generate firing pulses for their switches. One of the ways is to phase-shift or interleave the individual triangular carrier-waves from each other and space them equally over a switching cycle, so that some of the generated harmonics will cancel each other out and reduce the overall THD.

As a first example, when 2 converters operate in parallel, their carrier waves can be either (a) in-phase (b) out of phase by shifting them 180° from each other (Fig. 1.3a). This creates a situation that the aggregate harmonics generated in case (a) will be either doubled in magnitude based on the same fundamental frequency, or in case (b) they will be at same magnitude but at double the fundamental frequency. Case (b) is preferred since the aggregate harmonics can be filtered out much more economically.

As a second example, suppose there are 4 converters operating simultaneously (Fig. 1.3b). If the 4 converters operate in-phase, then the overall harmonics generated will be 4 times

the individual harmonics of one converter. However, if the 4 converters are interleaved and operate at 90° phase-shift to each other, the overall THD will be much reduced.

Similarly, if there are 8 converters active, the phase-shift of each converter will be 45° (Fig. 1.3c). The phase-shift θ is determined by $360^\circ/N$, where N is the number of converters.

Next, consider the situation where we have an EV charging station with N converter bays. During the day, the cars come and go randomly for charging i.e., there could be, at any given time, between 0 to N cars present. If there was communication from each bay to a central supervisory controller, then the interleaving of individual converters could be done appropriately. Without this communication system, it would not be possible to interleave the operation of the converters to reduce the overall THD.

The disadvantages of a communication system are the additional cost of sensors and telecommunications, latency or inherent time delays in the control loop, and reduction of reliability. Any break in the communication system would render the system inoperable.

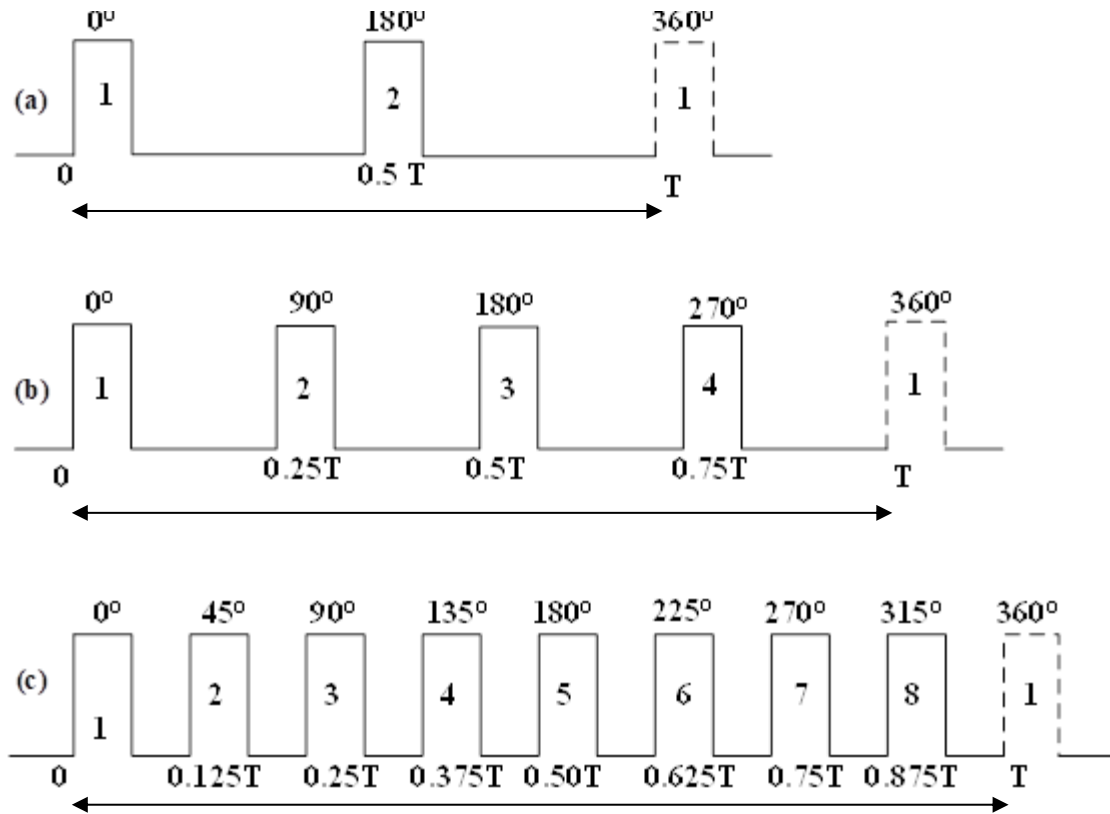


Figure 1. 3: Ideal phase shift when (a) two chargers (b) four chargers or (c) eight chargers operating in parallel.

Therefore, the following tasks are proposed for this research work:

1. To conduct a comprehensive literature study on impacts of fast charging of EVs on grid and state-of-the-art methods for reducing THD on the grid power.
2. To develop a Simulink model for a fast-charging station with the capability of charging 20 vehicles at a time.
3. To implement VSC and statistics-based control algorithm that requires no supervisory control or an external communication module, in the Simulink model of fast charging stations (FCS).
4. To study, compare and test the robustness of the system with and without the proposed algorithm when 5, 10, 15 and 20 cars are charged at a time.

Chapter 2. Literature review

2.1 Literature review

Several methods, techniques and control schemes have been proposed in the literature for reduction of harmonic distortion and optimization of the power quality. One of the most common methods is using filters. Both passive, active and hybrid filters have been widely used.

- Passive filters use passive elements such as capacitors and inductors which do not need an external power source. Commonly used passive filters include high-pass, low-pass, band-pass filter, and band-stop filters. Passive filters are inexpensive, but they can only compensate for a few selected harmonics. They cannot compensate the harmonics caused by dynamic changes of the harmonic distortion [9].
- Active filters, on the other hand, are of an analog/digital electronic filter type mostly used in high and variable supply of voltages. There are different configurations of active filters such as series-connected, parallel-connected and/or a combination of both. Active power filters remove harmonics by injecting power in series with the line. They electronically create and control reactive power to cancel out the harmonics. Although active filters are more effective and more energy efficient than the passive filters, active filters are more costly and complex than the passive filters. Reference [10] presents a comparison between active and passive filters used in 3-phase systems and concludes that the active filters outperform the passive filters.
- Hybrid filters combine active and passive filters and can be used for compensating harmonics and reactive power. Hybrid active/passive filter topologies are explored in [11] – [20] for reducing harmonics caused by different types of non-linear loads.

Similarly, an LCL filter combination is proposed for obtaining lowest harmonic distortion in [21]. A digital filter - Infinite Impulse Response (IIR) filter in [22] and Artificial Neural Network (ANN) controller - in [23] are proposed for harmonic reduction in grid connected system.

The phase-shifted switching cycles lead to variations of the output current ripples, which when summed together result in the minimization of ripples at the DC-link current. Reference [24] presents a technique for harmonic reduction using synchronized phase shifted parallel PWM inverters with current- sharing reactors in which optimum phase shift between parallel inverters with 3-level PWM yields minimum THD. High frequency sinusoidal PWM switching technique for harmonic reduction in a standalone/ utility grid have been proposed in [25]. DC-link shunt compensator with small DC-link capacitor have been proposed to reduce harmonics in single phase system, in [26] and [27]. Reference [28] uses a compensator consisting of a shunt active filter and a supercapacitor bank to compensate current harmonics of the nonlinear loads. Similarly, [29] proposes a multilevel shunt active power filter to compensate harmonic currents and reactive power in which three-phase bridge converters are connected to cascaded single-phase transformers. Hybrid D-STATCOM, consisting of a series capacitor with LCL filter, is used to compensate reactive power in non-linear loads in [30].

Reference [31] proposes phase shifting transformers in distribution systems for harmonics mitigation where “a combination of phase shifting transformers with 30 degrees apart, in a radial distribution system with similar harmonic spectrum and power, can get better results”. To mitigate the 5th and 7th and higher order harmonic currents, multiple transformers are required with a 30-deg relative phase shift between the two, connected to a common bus in an electrical distribution system. For example, one transformer with a zigzag configuration

harmonic mitigating transformer with a 0-deg phase shift, and the other transformers delta-wye with a 30-deg, -30-deg phase shift etc. are used [32]. Reference [33] proposes active power filter control using hybrid fuzzy proportional-integral and hysteresis controllers for mitigating the harmonics generated by Electric Vehicles. Reference [34] proposes a carrier-wave phase-shifting technique for minimizing the aggregate harmonics in networks of asymmetric parallel-connected inverters for distributed power generation system applications. This basically presents an optimization method for spacing carrier-wave phases to minimize harmonics in parallel-connected single-phase inverters. An optimal carrier phase spacing strategy for paralleled grid-connected converters with unequal terminal voltages is presented in [35]. In [33] - [35] a supervisory control or/and a communication line is required because the phase-shift is possible only when the angle is identified.

Several techniques have been proposed to reduce the aggregate harmonics on the grid because of unbalanced loads. References [36] - [42] present Interleaving techniques which are essentially carrier-wave phase-shifting techniques to reduce total harmonic distortions. There are two main types of interleaving methods that minimize grid harmonics: symmetric interleaving and asymmetric interleaving. Symmetric interleaving refers to equal carrier-wave phase-shifts that add to exactly one carrier cycle, that is, the carriers of N inverters are evenly spaced $360^{\circ}/N$ over a switching period. Asymmetric interleaving can also be further divided into regular asymmetric interleaving and irregular asymmetric interleaving. Like symmetric interleaving, asymmetric interleaving also has equal carrier-wave phase-shifts but unlike symmetric, regular asymmetric does not add to exactly one carrier cycle. In irregular asymmetric interleaving, the carrier-wave phase-shifts are not equal and, they do not add to one carrier cycle/ period. Reference [36] uses symmetric interleaving method to minimize the

grid harmonics in which PWM rectifiers are used. It uses two 3-phase rectifiers connected to the grid and thus carrier phases are shifted 180° apart. It also uses space vector modulation (SVM) with 60° clamping to reduce the switching losses and for power factor correction claiming 50% switching losses reduction by using it. In [37], the authors present a carrier-wave interleaving technique to minimize the grid current distortion when converters are connected in parallel. They propose an analytical method to estimate the optimal interleaving angle between identical converters with unequal terminal voltages. This works well if the network is identical and symmetric.

A comparison between symmetric and asymmetric interleaving is presented in [38] and by using double Fourier Series, it analytically shows that while symmetrical interleaving can cancel harmonic contents, the asymmetric interleaving is more useful in certain cases when EMI filter, DC-link capacitor ripple current and power losses are involved. Also, asymmetric interleaving can eliminate the total harmonic current at all frequencies. Further, this paper also proves that the by carrier-wave phase-shifting, the harmonics cancellation effects are the same even when the harmonics are injected into the PWM references. Asymmetric interleaving is also presented in [39] - [41] focusing on the aggregate harmonics' reduction in parallel-connected converters. A carrier-wave phase-shifting algorithm based on voltage and current measurements of each inverter is presented in [41], in which an iterative gradient method is used to update the carrier phase shift of each inverter. That is, it solves the minimization problem of $\theta^*c = \operatorname{argmin}D(\theta c)$. However, this algorithm is much more complex as it relies on reading the voltage and current harmonics which is cumbersome to calculate the harmonics. Also, the algorithm requires to keep changing the switching frequency of the inverter which is not very practical. Moreover, since each of the N inverters must iteratively perform the

component-wise update until the overall system reaches a steady-state carrier-wave phase spacing, it takes too long if there are many inverters in the system. Although [36] – [40] deal with symmetric and asymmetric methods to reduce harmonics, these all need some communication modules attached to them, thus making it hard to implement where extra communication devices are not available. In literature there are also some works in which harmonics are minimized using carrier-wave phase-shifting where communication modules between the converters are not required, but they are useful only for a few networks like two or three converters. References [41] and [42] present works where communication modules are not required, but they do not guarantee satisfactory harmonics reduction when many modules function at the same time.

A pulse train decomposition technique was developed in [43] to study the principle of harmonic cancellation among parallel 3-phase VSC modules. An insight gained from the analysis is that harmonic cancellation can occur not only between parallel VSC modules by interleaving, but also within individual modules due to periodic variation of certain harmonics (such as odd-order sideband harmonics around odd-order carrier-wave harmonics and even-order sideband harmonics around even-order carrier-wave harmonics when a triangle carrier-wave is used) over a fundamental cycle. Such periodically varying harmonics would appear to be cancelled when their average over a fundamental cycle is computed, such as in the case when Fourier analysis is applied over a fundamental cycle [44]. However, any nonlinear effects these harmonics produce on the source or the load, such as harmonic losses generated in filter capacitors and inductors, will not average out and cancel over a fundamental cycle.

A direct analysis of harmonic cancellation in modular 3-phase VSC was presented in [45]. The analytical phase voltage spectral model was developed by using the double Fourier

integral method [46]. Harmonic cancellation among parallel interleaved modules can be directly proven based on such closed-form functions. For N symmetrically interleaved three-phase VSC modules, it was proven in [45] that all carrier harmonics and their sideband components are cancelled except for those at multiples of N times the carrier frequency and their sideband harmonics. It was further shown that the harmonic cancellation effects not only exist in the phase voltages (differential- and common-mode) and currents, but also in the DC-link current. Therefore, there are many works done in the field of minimizing harmonics in the grid including using various kinds of filter, transformers, and even carrier-wave phase-shifting techniques. The closest to this research was a technique of carrier-wave phase-shifting, however, those works either use a communication module between the charging stations or the technique would work only for a small system with a few charging stations. This research work is quite different from the state-of-the-art in that this neither uses a communication module, nor a supervisory control. But, by using a knowledge of statistics, Carrier-wave phases are shifted using an algorithm that successfully minimizes grid harmonics to an acceptable level.

2.2 Motivation

As fast charging is the preferred method for EVs, the harmonic distortion due to power electronics used in converters needs to be maintained at a certain level, especially when many converters operate simultaneously in a fast-charging facility. As studied in the literature, one of the ways to reduce grid harmonics due to EV fast-chargers is to phase-shift the carrier-waves which essentially distributes the carrier-phases and thus the switching time of the converters is also distributed. As a result, some of the harmonics generated by the converters cancel each other out and THD is reduced. So, this research work is dedicated to devising a carrier phase-shifting method to maintain the grid power quality. Carrier phases can be easily

shifted if some sort of communication system is used between the station and the charging bays. In other words, the communication system can monitor the number of cars charging at any moment and depending on the number of cars charging, phases can be shifted by dividing the full cycle by the number of cars, for example, $360/N$. However, is it also possible to phase-shift the carrier-waves without using any communication between the bays and/or station? Using communication system has some cost, complication, and dependency on the communication module are associated with it. Moreover, using communication may not be feasible in some situations. So, this research devises a method to phase-shift carrier-waves using a statistical approach. By using the Poisson Distribution, the carrier-waves are distributed over time which then helps reduce the harmonics.

Chapter 3. The Proposed Approach

This chapter illustrates the carrier-wave phase-shifting process using the Poisson Distribution, a sample calculation, and the overall performance of the algorithm.

3.1 The proposed algorithm

This research proposes a new statistics-based algorithm in which converter carrier-waves are phase-shifted so that the generated converter harmonics are interleaved or distributed over a time-period and certain harmonics will cancel each other out. This will help maintain an overall lower level of harmonics. This technique does not require a supervisory centralized communication or information exchange system between individual converters/bays to coordinate the triangular carrier-waves for a charging station. The algorithm is implemented simultaneously in all the converters/bays and each bay shifts its carrier-wave phase independently, based on an algorithm that utilizes the Mean value (λ) of a Poisson Distribution

The process of calculating individual converter phase-shifts is explained in Fig.3.1. Since no centralized communication is used, the algorithm works by:

1. First, generating a normally distributed (Gaussian) random number to be the probability (Confidence Factor (CF)) for the Poisson Distribution.
2. Then, guessing the number of converters/bays (GN) active at any given moment based on probability. This is done by using the Inverse Poisson Distribution.
3. Next, guessing the position or order (GN) of a particular bay active at the given instant is calculated based on CF and GN, i.e., $GP = CF*GN$.
4. Finally, by calculating the phase-shift θ required for each converter (bay).

To determine the number of active converters at any given time, a statistical model is used which can make a good guess on the estimated number of converters active at any moment. The statistical model works if we know the Average Number of converters (λ) active during a particular period of the day; the day could be split into periods of low, medium, or high traffic etc. The average number of active converters can be predicted in one of several ways - like the load demand curve in a power system, or from previous experience, or from previous data etc.

3.2 Utilization of Poisson Distribution

3.2.1 Poisson Distribution

The Poisson Distribution helps to predict the probability of a given number of events occurring in a fixed interval of time if these events occur with a known constant average rate and independently of the time since the last event. In other words, the Poisson Distribution is valid if:

1. The average rate at which the events occur is known,
2. The occurrence of one event does not affect the probability that a second event will occur, i.e., the events occur independently and randomly.

For a random discrete variable X that follows the Poisson Distribution, the probability of x (within the lower x_{\min} and upper x_{\max} limits is given by:

$$P(X=x) = \frac{e^{-\lambda} \lambda^x}{x!} \quad (1)$$

Where,

$$x = x_{\min} \ 0, 1, 2, 3, \dots, x_{\max}$$

e is the Euler's number (e= 2.718)

λ is the average rate at which the events occur.

For example, if the average number of cars that charge at a charging station within 6 hours (say, between 6 am and 12 pm each day) is 15. What is the probability that 18 cars will charge the next day during the same time?

Using the formula,

$$P(X=18) = \frac{e^{-15} 15^{18}}{18!} = 0.0706 \text{ or } 7.06\%$$

So, the probability of 18 cars charging at the station within the next day is only 7.06%.

3.2.2 Cumulative Poisson Distribution

Like the Poisson Distribution, if the average rate at which the events occur is known for a fixed time interval, the Cumulative Poisson Distribution helps to predict the probability that an event occurs less than or equal to x times within that interval.

For example, if on average 5 cars charge at a charging station in 2 hours (say, between 9 am and 11 am), what is the probability that 0 to 3 cars (i.e., less than or equal to 3 cars) charge during the same time-period, the next day?

Here, we calculate the probabilities of 0 car charging, 1 car charging, 2 cars charging, and 3 cars charging and sum (accumulate) them all to get the Cumulative Poisson Distribution, i.e.,

$$P(X=0) = \frac{e^{-5} 5^0}{0!} = 0.0067$$

$$P(X=1) = \frac{e^{-5} 5^1}{1!} = 0.0336$$

$$P(X=2) = \frac{e^{-5}5^2}{2!} = 0.0842$$

$$P(X=3) = \frac{e^{-5}5^3}{3!} = 0.1403$$

Therefore, $P(X \leq 3) = 0.6737 + 0.0336 + 0.0842 + 0.14037 = 0.26$ or 26%

So, the probability that less than or equal to 3 cars charging within the next day is 26%.

3.2.3 Inverse Poisson Distribution

The Inverse Poisson Distribution is used to find the Average number λ if the probability is known, for a fixed interval of time.

For example, if the probability that at least one car charges at a given time interval is 90%, what is the average rate at which the cars charge during the same time interval?

Here,

$$P(X \geq 1) = 0.9$$

$$P(X = 0) = 1 - P(X \geq 1) = (1-0.9) = 0.1$$

$$P(X=0) = e^{-\lambda} \frac{\lambda^0}{0!}$$

Hence, $\lambda = 2.3$

Now, note that since λ must be an integer, it is rounded off to the nearest integer. So, the average number of cars charging at the given time is 2.

As seen above, calculating the Poisson Distribution, the Cumulative Poisson Distribution or Inverse Poisson Distribution manually can be cumbersome. So, the usual way

to calculate the variants of Poisson Distribution is to use software like MATLAB which has a $poissinv(P,\lambda)$ function

3.3 Carrier wave phase shift calculation using Poisson Distribution

Figure 3.1 illustrates the implementation of the algorithm using MATLAB Simulink. The Guessed Number of active bays (GN) is obtained from the Inverse Poisson Distribution function by inputting the values of λ and CF. The function also multiplies the CF and GN, rounds the product to its nearest integer and outputs the Guessed Position (GP) of a particular converter. GP is the guessed order of the converter among the active converters at that instant of time. In other words, GP determines if it is the 5th bay that is active now or the 6th bay or the 7th bay and so on. Although the guessed position is also random and it may not locate the exact position since it is based on the random probability, the GP still helps make the phase-shift more distributed as the carrier-wave phase-shift is calculated based on this. Then, equation (2) is used to calculate the converter triangular carrier-wave phase-shift (θ). Finally, using the converter triangular carrier-wave signal (TSC), and the calculated phase-shift (θ) the resultant phase-shifted triangular carrier signal (STCS) is fed to the corresponding Voltage Source Converter (VSC).

$$\text{Phase shift } (\theta) = \frac{GP}{GN*F_c} \quad (2)$$

Where, converter triangular carrier wave frequency ($F_c = 1.98$ kHz) is chosen as an integer multiple of the fundamental frequency i.e., $33*60$ Hz; this multiple must be high enough to filter out the harmonics generated by the VSC.

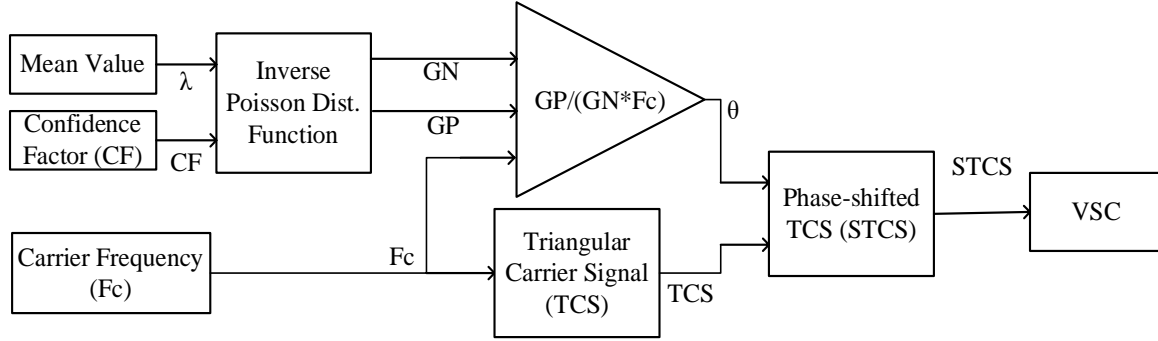


Figure 3. 1: Carrier wave phase shift calculation algorithm

For a sample phase-shift calculation, the Cumulative Poisson Distribution is plotted (Fig. 3.2) from which, a random probability CF is picked and then the corresponding GN is obtained based on the graph. The CF and GN are then multiplied to determine the GP of a particular bay/converter for that instant. Finally, triangular carrier-wave phase-shift (θ) is calculated using equation (2). Table 3.1 shows the sample calculations for a triangular carrier wave phase shift θ considering the constant average rate $\lambda = 15$.

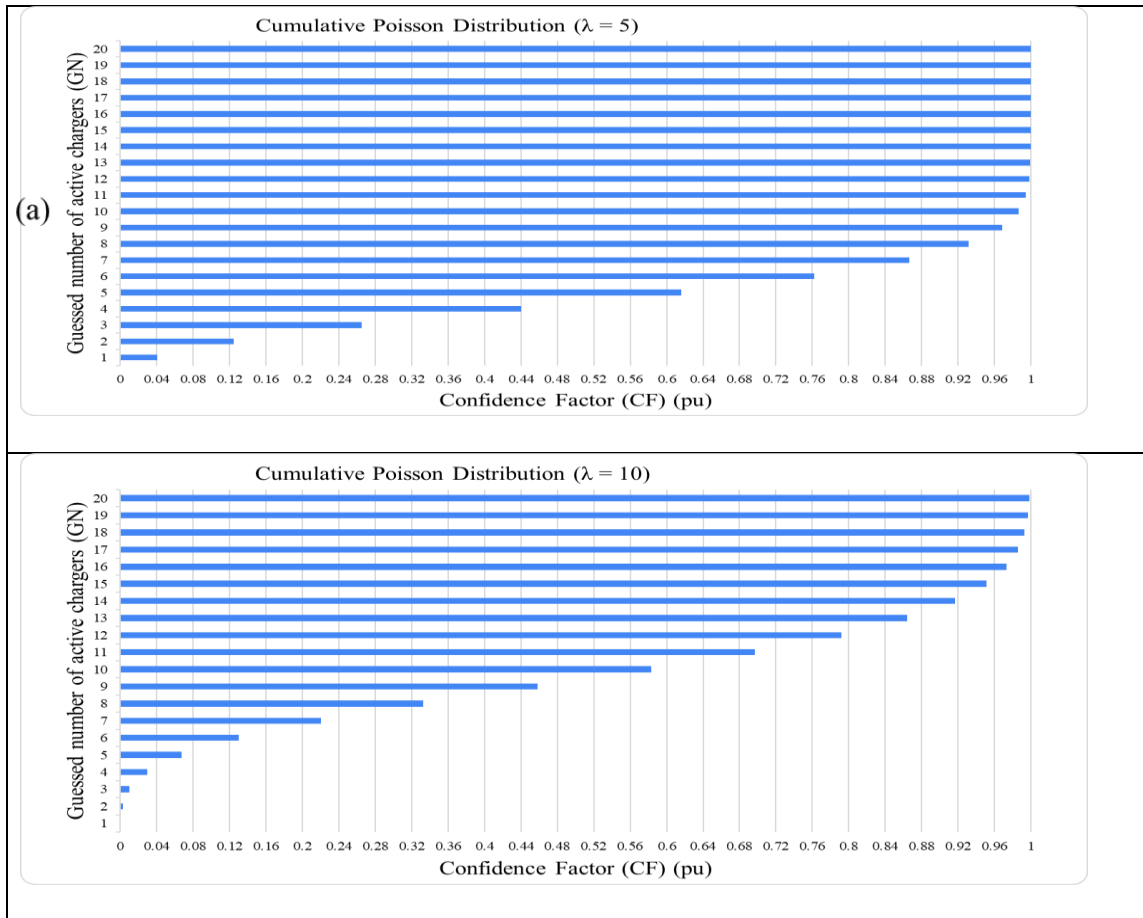
One of the main assumptions in this research is that the charging station has already carried out load flow studies based on load forecasts on a day-ahead basis. And that the charging station has sufficient data as to how much power is required each day, including at specific times of the day.

A full day can be divided into several specific time-periods such as low-traffic, medium-traffic, and high-traffic periods. As the charging station is busier during certain periods of the day and less busy during other periods, the following scenario is assumed:

- Low-traffic period – Only 5 out of 20 chargers are active,
- Medium-traffic period – only 10 out of 20 chargers are active,
- High-traffic period – All 20 out of 20 chargers are active.

Figure 3.2 shows the Cumulative Poisson Distribution graphs for three mean values which represent different time periods in a day. Figures 3.2a, b, c represent these three scenarios where $\lambda = 5, 10, 15$ respectively.

Based on the Cumulative Poisson Distribution graph of Figure 3.2c, phase-shifts for 20 converters in the charging station are calculated in Table 3.1 for $\lambda = 15$. In Table 3.1, since the GP needs to be an integer number, the actual GP (GP_{actual}) is rounded to the nearest integer number. Similar tables may be generated for values of $\lambda = 5$ or 10, corresponding to low or medium traffic periods respectively.



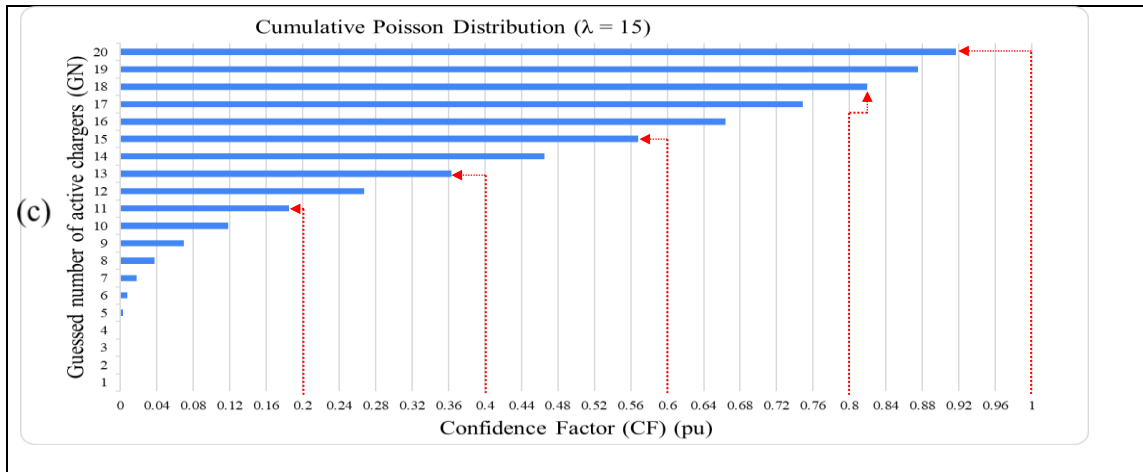


Figure 3. 2: Cumulative Poisson Distribution for $\lambda = 5, 10$ and 15

Similar tables may be generated for values of $\lambda = 5$ or 10 , corresponding to low or medium traffic periods respectively.

Figure 3.3 shows the converter triangular carrier-wave signals (frequency of 1.98 kHz and amplitude of ± 1). The first wave (color black) is the reference phase of 0 degrees. The second wave (color green) is a phase-shift of 65 degrees. The third wave (color blue) and the fourth wave (color orange) are the phase-shifts of 138 degrees and 216 degrees respectively. Similarly, the fifth wave (color red) is 280 degrees phase-shift, and the sixth wave (color purple) is a 360 degrees phase shift. Note that in Figure 3.3, only 5 waves are shown from the full list shown in Table 3.1; this is intentional to not crowd the figure.

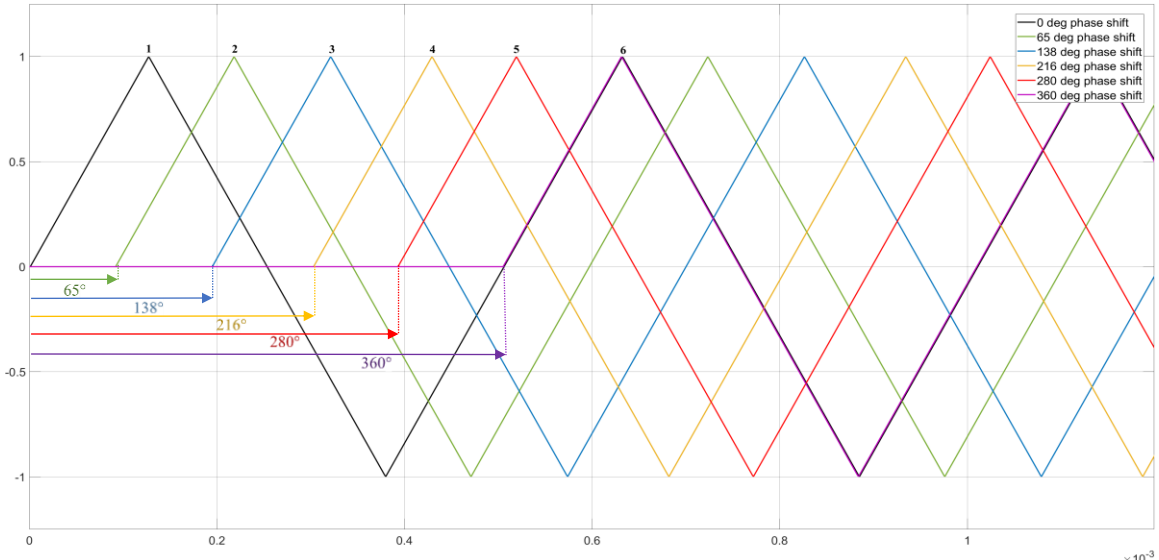


Figure 3. 3: Triangular carrier waveforms showing the calculated phase-shift for 6 selected cases (shaded rows) from Table 3.1

Table 3. 1: Phase shifts calculation for $\lambda = 15$

CF	GN	GP ($GP_{\text{actual}}=CF*GN$)	GP [GP]	θ in ms ($\theta=\frac{GP}{GN*Fc}$)	θ in deg
0.04	8	0.32	0	0	0
0.08	9	0.72	1	0.0561	40
0.12	10	1.20	1	0.0505	36
0.16	11	1.76	2	0.0918	65
0.20	11	2.20	2	0.0918	65
0.24	12	2.88	3	0.1263	90
0.28	12	3.36	3	0.1263	90
0.32	13	4.16	4	0.1554	111
0.36	13	4.68	5	0.1943	138
0.40	13	5.20	5	0.1943	138
0.44	14	6.16	6	0.2165	154
0.48	14	6.72	7	0.2525	180
0.52	15	7.80	8	0.2694	192
0.56	15	8.40	8	0.2694	192
0.60	15	9.00	9	0.3030	216
0.64	16	10.24	10	0.3157	225
0.68	16	10.88	11	0.3472	248
0.72	17	12.24	12	0.3565	254
0.76	17	12.92	13	0.3862	275
0.80	18	14.40	14	0.3928	280
0.84	18	15.12	15	0.4209	300
0.88	19	16.72	17	0.4519	322
0.92	20	18.40	18	0.4545	324
0.96	20	19.20	19	0.4798	342
1.00	20	20.00	20	0.5051	360

This calculation of phase-shift shows how the phases of the carrier-waves can be systematically shifted by using the statistical model.

3.4 Discussion, Results and Simulation

A MATLAB/Simulink model is used to verify the effectiveness of the proposed algorithm. Grid voltage THD values are compared for two cases: one, when no algorithm is used and the other, when the proposed algorithm is used. For simplicity, the grid voltage THDs are observed for four scenarios:

1. When only 5 out of 20 charging bays are active; results are shown in Figure 3.4a,
2. When only 10 out of 20 charging bays are active; results are shown in Figure 3.4b,
3. When only 15 out of 20 charging bays are active; results are shown in Figure 3.4c and
4. When all 20 charging bays are active; results are shown in Figure 3.4d.

Figure 3.4 illustrates the differences between the two cases: when no algorithm is used and when the proposed algorithm is used. These differences are presented in terms of the grid voltage and current wave forms and THDs in the grid voltages. The left column presents the results obtained when no algorithm is used. The right column presents the results when the proposed algorithm is used.

Figure 3.4a compares the results between the two cases when only 5 out of 20 charging bays are active. In this case, not only are the voltage and current wave forms improved, the THD in grid voltage is also reduced from 6.07% when no algorithm is used to 2.81% when the proposed algorithm is used.

Similarly Figure 3.4b shows that the use of the algorithm reduces the grid harmonics from 11.38% to 3.29% when 10 out of 20 charging bays are active.

Figure 3.4c shows that the noisy wave forms from the normal case are improved greatly by using the algorithm, reducing the voltage THD from 15.98% to 5.23%.

The algorithm is effective for the last scenario also when all the 20 charging bays are active (Fig. 3.4d). The wave forms are significantly improved and the THD in the grid voltage is reduced from 20.10% to 5.63%.

Figure 3.5 shows the benchmark situation when the carrier-wave phases are ideally shifted by means of communication between the station and bays or some supervisory control. In this ideal situation, the THDs are optimally reduced. The results in the three cases can be compared: (a) when no algorithm is used, (b) when the algorithm is used and (c) the benchmark case.

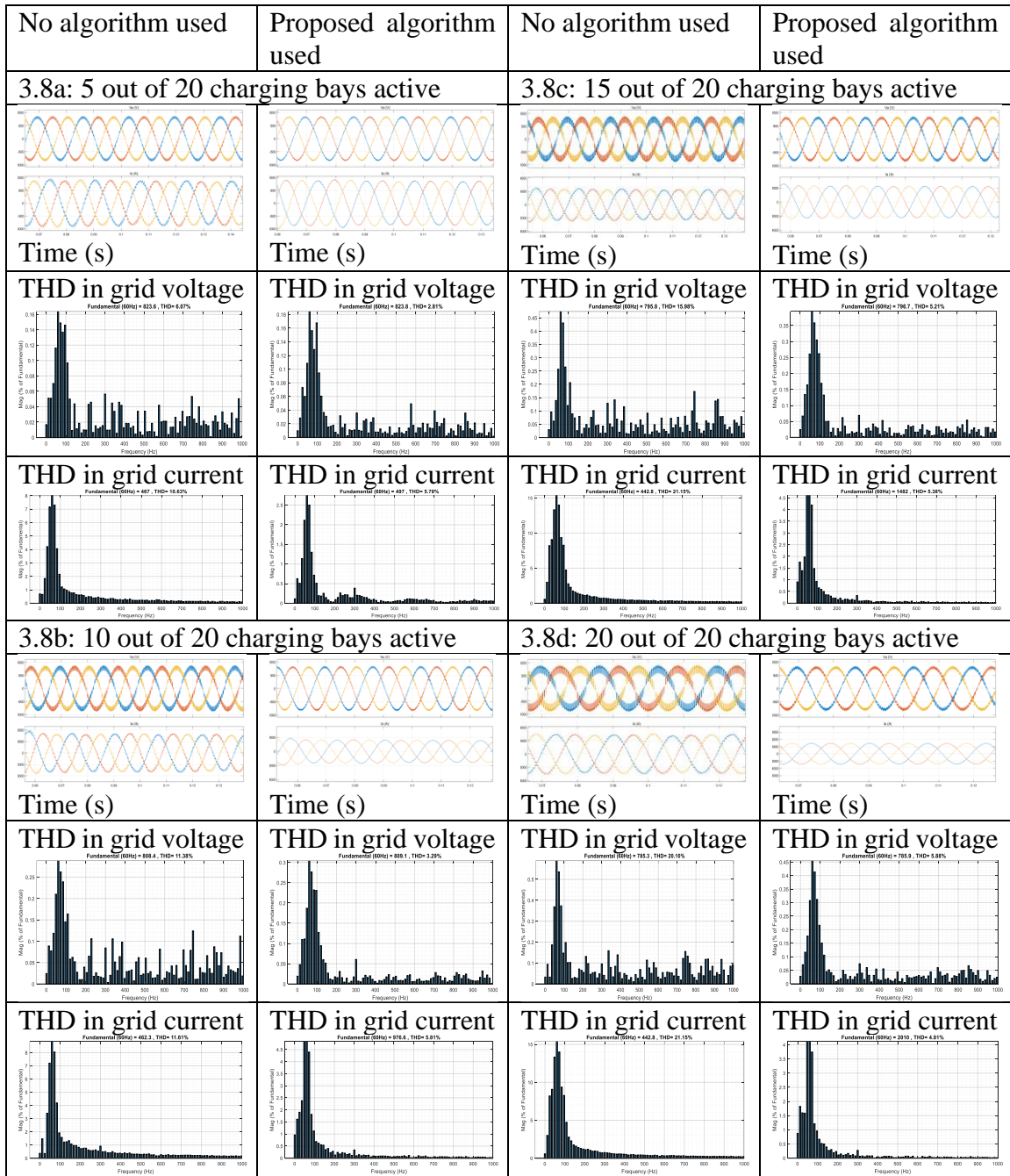


Figure 3. 4: Harmonic profiles and harmonic distortion in grid voltage and grid current

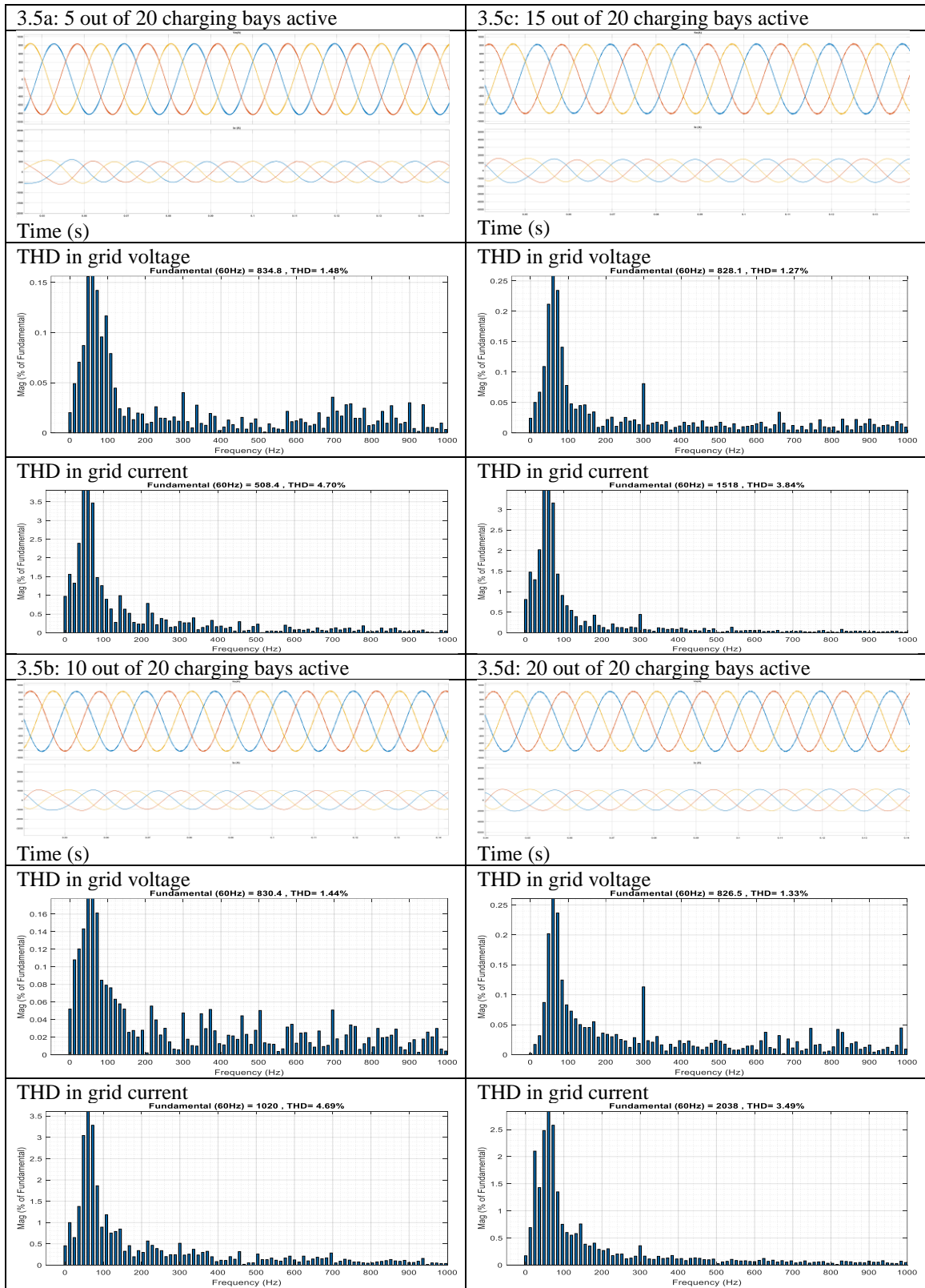


Figure 3. 5: Benchmark harmonic profiles and harmonic distortion in grid voltage and current

Table 3.2 and Figures 3.6 and 3.7 show the performance summary for the three cases. In figures 3.6 and 3.7, the vertical axes represent the THD (%), and the horizontal axes represent the number of active charging bays. As can be seen, the use of the algorithm significantly reduces the grid harmonics caused by the charging station. The proposed algorithm effectively maintains the level of harmonics in the grid even when all 20 EVs are charging simultaneously. The THD in grid voltage is maintained at 5.63% which is almost one fourth reduction from the normal case when no algorithm is used. For the same situation, the voltage THD could ideally be reduced to 1.33%. Similarly, THD in current harmonics is also maintained at 5.81% in the worst-case scenario. The ideal phase-shift in this scenario would reduce the THD_I to 3.49%. It is noteworthy that when only 5 cars charge simultaneously, THD_V is 6.07% when the algorithm is not used and 3.09% when the algorithm is used, i.e., the harmonics is reduced by almost half. However, when 20 cars charge simultaneously, the THD_V is reduced almost 4 times which is because as more converters are active, there is more phase shift among the converters, which means more harmonics cancellation. Similarly, if the carrier phases were distributed evenly, there could be even more harmonics cancellation and it would further minimize the THDs. The proposed paper depicts the situation where communication module is not desired for various reasons such as cost, feasibility etc., yet it performs well enough to maintain the power quality to an accepted level.

The algorithm is tested for the worst-case scenario for all level of SOC of the batteries. As long as the data is realistic, the algorithm performs very well by reducing the harmonics. Figure 3.2 shows the THD for different SOC of the batteries. For example, if the data shows that at a certain time of the day, only 5 vehicles charge, the algorithm shifts phases of the carrier waves irrespective of the state of charge levels in the batteries. However, suppose the

data shows that average rate of EVs charging at a certain day is 10 cars, but only one car charges at that time, then it is a bad data collection, and it will be obvious for the algorithm to not perform sufficiently.

Table 3. 2: THD results summary

Number of active chargers (bays)	No algorithm		Using algorithm with constant SOCs		Using algorithm with different SOCs		Ideal phase shift	
	THD _v	THD _i	THD _v	THD _i	THD _v	THD _i	THD _v	THD _i
5	6.07	10.03	3.09	5.78	3.06	5.75	1.48	4.70
10	11.38	11.61	3.22	5.81	3.43	5.61	1.44	4.69
15	15.98	21.15	5.23	5.38	5.29	5.95	1.24	3.84
20	20.1	21.15	5.63	4.81	5.35	5.96	1.33	3.49

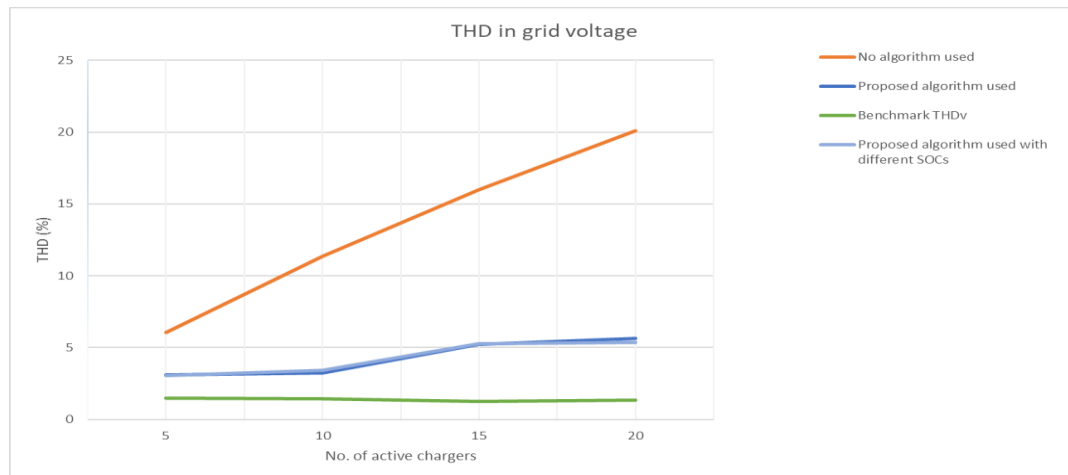


Figure 3. 6: Results summary for grid voltage

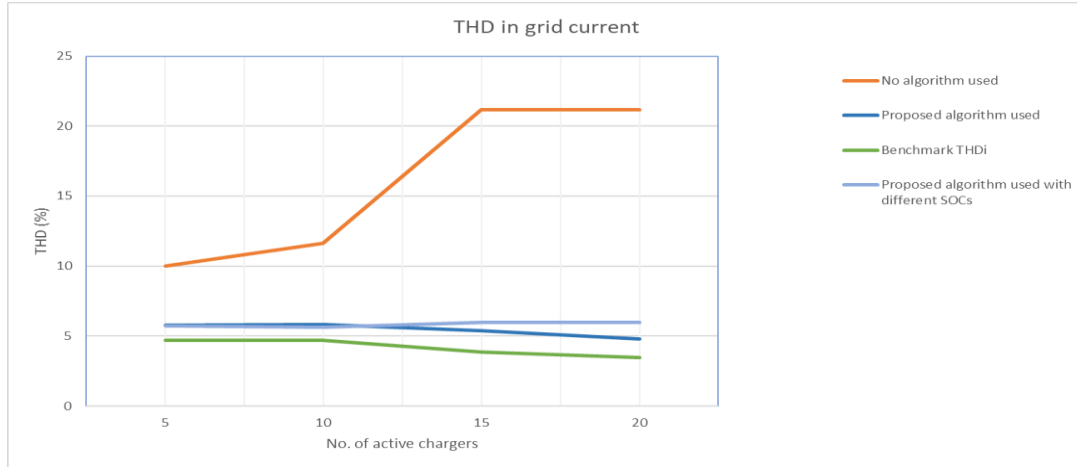


Figure 3. 7: Results summary for grid current

Chapter 4. System Description and the control mechanism

The overall system configuration used for testing the algorithm is shown in Figure 4.1. The system consists of a 60 kW 3-phase 13.8 kV grid system, a 13.8 kV/600 V step-down transformer, a 3-phase AC-DC converter and a bidirectional buck-boost DC-DC converter. A source impedance of 16.58 μH inductor and 89.29 $\text{m}\Omega$ resistor are used in series. This system also includes an RL- AC filter which includes a resistor of 1 $\text{m}\Omega$ and an inductor of 3 μH connecting between each phase AC and AC-DC converter necessary to boost DC output to maintain the DC bus voltage at 600 V [47]. For the load, lithium-ion batteries with the nominal voltage of 600 V and 16.67 Ah rated capacity are used.

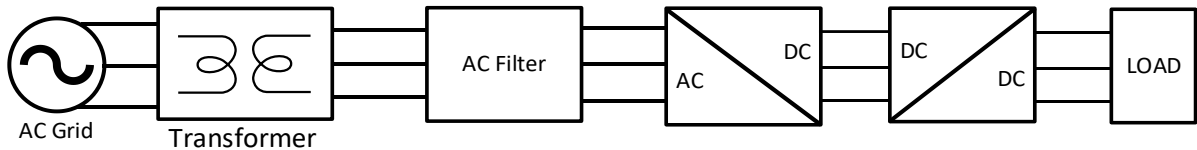


Figure 4. 1: System representation

The proposed methodology is implemented using Simulink platform to study and validate the model performance as illustrated in Figure 4.2. To depict a practical scenario, this experiment is done with 20 bays at a charging station connected to the grid and each charging bay consists of VSC control and carrier phase shift mechanism as shown in Figure 4.3. Details of each component are given in the next section.

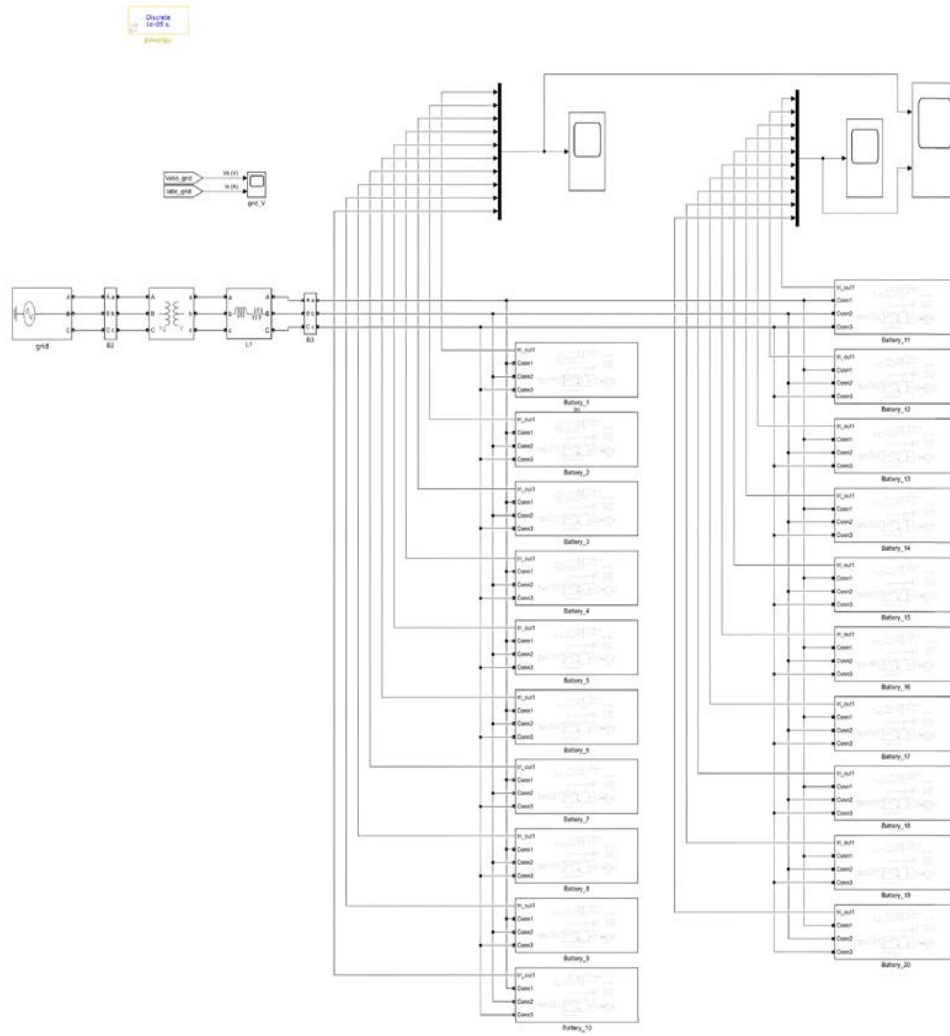


Figure 4. 2: Simulink model of the system with 20 bays

Since there is no communication module used to communicate between and among the charging bays, so there is no supervisory control needed, and the algorithm is independently implemented in each bay station. Thus, each bay station consists of the algorithm that shifts the carrier-wave phase and VSC control to generate gate pulses for the DC-DC converter. Figure 4.3 shows the configuration of each charging bay.

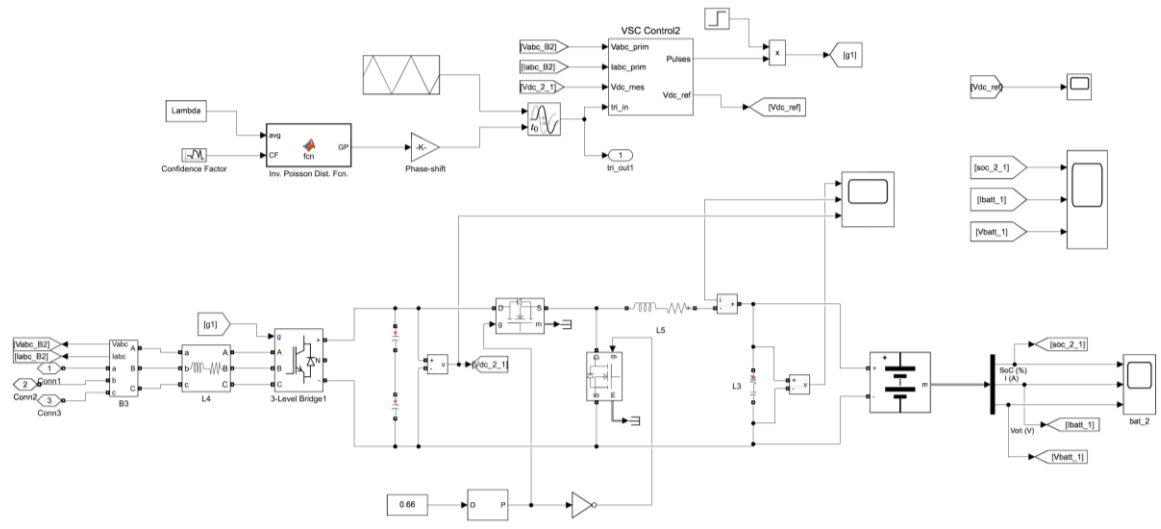


Figure 4. 3: Control mechanism of a charging bay consisting of carrier phase shift algorithm, VSC control and DC-DC converter.

Chapter 5. Conclusions

5.1 Conclusion Summary

The focus of this study was mainly on how grid harmonics can be minimized when several cars charge simultaneously at a fast-charging facility. The contribution of this work is in the reduction of grid harmonics without using any additional filters or transformers and without any communication requirements between the charging bays. The following is the summary obtained by this study:

- Grid harmonics caused by fast EV chargers can be minimized without using additional filters or transformers.
- Harmonics can be reduced by applying a knowledge of statistics to shift the phases of carrier-waves of the individual converters/bays.
- By shifting the phases of carrier-waves, the transient ripples caused by the converters are evenly distributed over a period. This way, certain harmonics cancel each other out and the overall THD is reduced.
- There are several ways of shifting phases of carrier-waves; however, the most practical and feasible way that performs well even when multiple vehicles are connected to the grid for charging is by implementing the algorithm in each of the charging bays.
- Implementing the algorithm in each converter does not require any communication module to communicate between and among the charging bays. Thus, this algorithm avoids the need for any centralized supervisory control.
- This algorithm is implemented in a scenario when a charging facility consists of 20 charging bays, and the overall THD is reduced from 20.10% to 5.88% in the worst

scenario when all 20 charging bays are charging. This algorithm, as the results show, can reduce harmonics to one-third even in the worst-case scenario.

5.2 Future scope

The work provides more opportunities to carry on further research:

- The focus of this research is only on how to reduce grid harmonics caused by EV chargers with the assumption that the charging station has sufficient capacity to charge EVs from its charging bays. A future study can consider how to respond to the issues that may arise from insufficient capacity at the sub-station caused by undervoltage or power congestion or power quality related issues.
- This research is restricted to transferring power from grid to vehicle. A further study on how to reduce grid harmonics when power is from vehicle to grid can also be looked at. The vehicle batteries can charge and store power during off-peak times and the power can be supplied back to the grid in peak times.
- This work was limited to considering different scenarios such as the harmonic distortion levels when no algorithm is used, the effectiveness of the use of the algorithm to reduce the harmonic distortion levels and the benchmark results that can be obtained by using a communication module.
- The work reported here is only covering a simulation model. However, an experimental work can be carried out by building a hardware model to implement the algorithm in the real-world scenario. This can be done in several ways: by scaling down the model and implementing it in the lab, or by using the available real-time Hardware-in-the-loop equipment in the university labs such as LabVolt simulator, OCPP Simulation Software etc. However, due to time constraints, this was left as future work.

- This research is only focused on reducing grid harmonics by phase shifting carrier waves. However, the research can be further extended incorporating many other power quality issues such as voltage sags, undervoltage, fault protection etc.
- A comparative study can be performed to see the results in terms of performance and costs by using this algorithm and by using a supervisory control using communication modules.

REFERENCES

- [1] IEA, Global electric passenger car stock, 2010-2020, IEA, Paris
<https://www.iea.org/data-and-statistics/charts/global-electric-passenger-car-stock-2010-2020>
- [2] Hydro Quebec, “Electric Vehicle Charging Stations-Technical Installation Guide”, Hydro Quebec, ETS, [online] Available:
<http://www.hydroquebec.com/data/electrification-transport/pdf/technical-guide.pdf>.
- [3] Charge Point, “Driver’s Checklist: A Quick Guide to Fast Charging”, [online] Available: https://www.chargepoint.com/files/Quick_Guide_to_Fast_Charging.pdf
- [4] Doug Kettles, “Electric Vehicle Charging Technology Analysis and Standards”, Electric Vehicle Transportation Centre, February 2015.
- [5] M. J. Rutherford and V. Yousefzadeh, “The impact of Electric Vehicle battery charging on distribution transformers,” 2011 Twenty-Sixth Annual IEEE Applied Power Electronics Conference and Exposition (APEC), 2011, pp. 396-400, doi: 10.1109/APEC.2011.5744627.
- [6] M. K. Gray and W. G. Morsi, “Power Quality Assessment in Distribution Systems Embedded with Plug-In Hybrid and Battery Electric Vehicles,” IEEE Transactions on Power Systems, vol. 30, no. 2, pp. 663-671, March 2015, doi: 10.1109/TPWRS.2014.2332058.
- [7] L. Pieltain Fernández, T. Gomez San Roman, R. Cossent, C. Mateo Domingo and P. Frías, “Assessment of the Impact of Plug-in Electric Vehicles on Distribution Networks,” IEEE Transactions on Power Systems, vol. 26, no. 1, pp. 206-213, Feb. 2011, doi: 10.1109/TPWRS.2010.2049133.

- [8] "IEEE Standard for Harmonic Control in Electric Power Systems," *IEEE Std 519-2022 (Revision of IEEE Std 519-2014)*, vol., no., pp.1-31, 5 Aug. 2022, doi: 10.1109/IEEESTD.2022.9848440.
- [9] L. Motta and N. Faúndes, "Active / passive harmonic filters: Applications, challenges & trends," 2016 17th International Conference on Harmonics and Quality of Power (ICHQP), 2016, pp. 657-662, doi: 10.1109/ICHQP.2016.7783319.
- [10] J. Aswal and Y. Pal, "Passive and active filter for harmonic mitigation in a 3-phase, 3-wire system," 2018 2nd International Conference on Inventive Systems and Control (ICISC), 2018, pp. 668-672, doi: 10.1109/ICISC.2018.8398882.
- [11] J. Aswal and Y. Pal, "Harmonic Mitigation in a 3-Phase, 3-Wire System Using Hybrid Filter," 2018 2nd International Conference on Trends in Electronics and Informatics (ICOEI), 2018, pp. 743-746, doi: 10.1109/ICOEI.2018.8553776.
- [12] D. Suresh and S. Singh, "Reduced rating hybrid active power filter in a three-phase four-wire distribution system," 2014 International Conference on Computer Communication and Informatics, 2014, pp. 1-5, doi: 10.1109/ICCCI.2014.6921839.
- [13] A. Moeini, S. Wang, B. Zhang and L. Yang, "A Hybrid Phase Shift-Pulsewidth Modulation and Asymmetric Selective Harmonic Current Mitigation-Pulsewidth Modulation Technique to Reduce Harmonics and Inductance of Single-Phase Grid-Tied Cascaded Multilevel Converters," *IEEE Transactions on Industrial Electronics*, vol. 67, no. 12, pp. 10388-10398, Dec. 2020, doi: 10.1109/TIE.2019.2959499.
- [14] D. Bharat and P. Srivastava, "Removal of source current harmonics under Harmonically Balanced Condition using shunt hybrid active filters," 2016 IEEE 1st

- International Conference on Power Electronics, Intelligent Control and Energy Systems (ICPEICES)*, 2016, pp. 1-6, doi: 10.1109/ICPEICES.2016.7853153.
- [15] M. P. Nandankar and D. S. More, "Performance analysis of transformer-less hybrid active power filter using different inverter topologies," *2017 International Conference on Intelligent Computing, Instrumentation and Control Technologies (ICICICT)*, 2017, pp. 892-897, doi: 10.1109/ICICICT1.2017.8342683.
- [16] T. Lee, Y. Wang and J. Li, "Design of a hybrid active filter for harmonics suppression in industrial facilities," *2009 International Conference on Power Electronics and Drive Systems (PEDS)*, 2009, pp. 121-126, doi: 10.1109/PEDS.2009.5385811.
- [17] M. Jalil and A. Amiri, "An Effective Structure of Three-Phase Parallel Hybrid Active Power Filter to Accurate Harmonic Elimination," *2020 15th International Conference on Protection and Automation of Power Systems (IPAPS)*, 2020, pp. 123-129, doi: 10.1109/IPAPS52181.2020.9375544.
- [18] V. H. A, P. R. B. V, P. V, K. B. S and T. S, "Mitigation of Harmonics at the AC Mains Connected to Nonlinear Loads using Hybrid Power Filters," *2020 IEEE Bangalore Humanitarian Technology Conference (B-HTC)*, 2020, pp. 1-6, doi: 10.1109/B-HTC50970.2020.9297881.
- [19] D. Daftary and M. T. Shah, "Design and Analysis of Hybrid Active Power Filter for Current Harmonics Mitigation," *2019 IEEE 16th India Council International Conference (INDICON)*, 2019, pp. 1-4, doi: 10.1109/INDICON47234.2019.9029052.
- [20] S. Senini and P. J. Wolfs, "Hybrid active filter for harmonically unbalanced three phase three wire railway traction loads," *IEEE Transactions on Power Electronics*, vol. 15, no. 4, pp. 702-710, July 2000, doi: 10.1109/63.849040.

- [21] E. E. Ahsan, M. A. Shobug, M. M. H. Tanim and M. H. Reza, "Harmonic Distortion Reduction of Transformer less Inverter's Output Voltage Using 5-Level Single-Phase Inverter and LCL Filter," 2nd International Conference on Advanced Information and Communication Technology (ICAICT), 2020, pp. 251-256, doi: 10.1109/ICAICT51780.2020.9333510.
- [22] A. Sinha and S. B. Singh, "Modelling and Simulation of Grid Connected PV System for Harmonic Reduction by Using Digital Filter," First IEEE International Conference on Measurement, Instrumentation, Control and Automation (ICMICA), 2020, pp. 1-5, doi: 10.1109/ICMICA48462.2020.9242724.
- [23] O. Hemakesavulu, M. S. Sandeep and C. S. Durganjali, "ANN controller for harmonic reduction in grid connected system," 2016 International Conference on Communication and Electronics Systems (ICCES), 2016, pp. 1-6, doi: 10.1109/CESYS.2016.7889948.
- [24] N. Benaifa, H. Bierk, A. H. M. A. Rahim and E. Nowicki, "Analysis of Harmonic Reduction for Synchronized Phase-shifted Parallel PWM Inverters with Current Sharing Reactors," 2007 IEEE Canada Electrical Power Conference, 2007, pp. 134-139, doi: 10.1109/EPC.2007.4520319.
- [25] A. Z. M. S. Muttalib, S. M. Ferdous, A. M. Saleque, N. M. A. Hasan and M. M. Chowdhury, "Design and simulation of an inverter with high frequency sinusoidal PWM switching technique for harmonic reduction in a standalone/ utility grid synchronized photovoltaic system," International Conference on Informatics, Electronics & Vision (ICIEV), 2012, pp. 1168-1173, doi: 10.1109/ICIEV.2012.6317533.

- [26] S. Y. C and P. S, "Reduction of Harmonics using DC-link Shunt Compensator in Single Phase Grid Connected Motor Drive System," International Conference on Electrical, Electronics, Communication, Computer, and Optimization Techniques (ICEECCOT), 2018, pp. 1306-1308, doi: 10.1109/ICEECCOT43722.2018.9001621.
- [27] H. Shin, Y. Son and J. -I. Ha, "Grid Current Shaping Method with DC-Link Shunt Compensator for Three-Phase Diode Rectifier-Fed Motor Drive System," IEEE Transactions on Power Electronics, vol. 32, no. 2, pp. 1279-1288, Feb. 2017, doi: 10.1109/TPEL.2016.2540651.
- [28] A. Virtanen and H. Tuusa, "Power compensator for high power fluctuating loads with a supercapacitor bank energy storage," IEEE 2nd International Power and Energy Conference, 2008, pp. 977-982, doi: 10.1109/PECON.2008.4762615.
- [29] G. A. de Almeida Carlos, C. B. Jacobina, J. P. R. A. Mello and E. C. dos Santos, "Shunt active power filter based on cascaded transformers coupled with three-phase bridge converters," IEEE Applied Power Electronics Conference and Exposition (APEC), 2016, pp. 2720-2726, doi: 10.1109/APEC.2016.7468248.
- [30] S. Darade and P. C. Tapre, "Compensation of Reactive Power in Non-Linear Loads Using Hybrid DSTATCOM Topology," IEEE International Conference on System, Computation, Automation and Networking (ICSCA), 2018, pp. 1-5, doi: 10.1109/ICSCAN.2018.8541229.
- [31] Gabriel Malagon Carvajal, Gabriel Ordonez Plata, Wilson Giraldo Picon and Julio Cesar Chacon Velasco, "Investigation of phase shifting transformers in distribution systems for harmonics mitigation," 2014 Clemson University Power Systems Conference, 2014, pp. 1-5, doi: 10.1109/PSC.2014.6808119.

- [32] A. Ahmad, R. Omar and M. Sulaiman, "Application of ZigZag Transformers to Mitigate Triplen Harmonics in 3 Phase 4 Wire Electrical Distribution System," 2006 4th Student Conference on Research and Development, 2006, pp. 266-269, doi: 10.1109/SCORED.2006.4339351.
- [33] F. R. Puthiyottil, H. Shareef and K. S. P. Kiranmai, "Active Power Filter Control Using Hybrid Fuzzy Proportional-Integral and Hysteresis Controllers for Mitigating the Harmonics Generated by Electric Vehicles," 2020 IEEE International Conference on Power and Energy (PECon), 2020, pp. 13-18, doi: 10.1109/PECon48942.2020.9314524.
- [34] J. Poon, B. Johnson, S. V. Dhople and J. Rivas-Davila, "Decentralized Carrier Phase Shifting for Optimal Harmonic Minimization in Asymmetric Parallel-Connected Inverters," IEEE Transactions on Power Electronics, vol. 36, no. 5, pp. 5915-5925, May 2021, doi: 10.1109/TPEL.2020.3030009.
- [35] J. S. Siva Prasad and G. Narayanan, "Minimization of Grid Current Distortion in Parallel-Connected Converters Through Carrier Interleaving," IEEE Transactions on Industrial Electronics, vol. 61, no. 1, pp. 76-91, Jan. 2014, doi: 10.1109/TIE.2013.2245620.
- [36] Kun Xing, F. C. Lee, D. Borrojevic, Zhihong Ye, and S. Mazumder, "Interleaved PWM with discontinuous space-vector modulation," IEEE Trans. Power Electron., vol. 14, no. 5, pp. 906–917, Sep. 1999.
- [37] J. S. Siva Prasad and G. Narayanan, "Minimization of grid current distortion in parallel-connected converters through carrier interleaving," IEEE Trans. Ind. Electron., vol. 61, no. 1, pp. 76–91, Jan. 2014.

- [38] T. Beechner and J. Sun, "Harmonic cancellation under interleaved PWM with harmonic injection," in Proc. IEEE Power Electron. Specialists Conf., Jun. 2008, pp. 1515–1521.
- [39] T. Beechner and J. Sun, "Asymmetric interleaving—a new approach to operating parallel converters," in Proc. IEEE Energy Convers. Congr. Expo., Sep. 2009, pp. 99–105.
- [40] C. Casablanca and J. Sun, "Interleaving and Harmonic Cancellation Effects in Modular Three-Phase Voltage-Sourced Converters," IEEE Workshops on Computers in Power Electronics, 2006, pp. 275-281, doi: 10.1109/COMPEL.2006.305626.
- [41] J. Poon, B. Johnson, S. V. Dhople and J. Rivas-Davila, "Decentralized Carrier Phase Shifting for Optimal Harmonic Minimization in Asymmetric Parallel-Connected Inverters," IEEE Transactions on Power Electronics, vol. 36, no. 5, pp. 5915-5925, May 2021, doi: 10.1109/TPEL.2020.3030009.
- [42] M. Sinha, J. Poon, B. B. Johnson, M. Rodriguez, and S. V. Dhople, "Decentralized interleaving of parallel-connected buck converters," IEEE Trans. Power Electron., vol. 34, no. 5, pp. 4993–5006, May 2019.
- [43] C. Casablanca and J. Sun, "Interleaving and harmonic cancellation effects in modular three-phase voltage-sourced converter," Proc. COMPEL'06, July 2006.
- [44] D. G. Holmes and T. A. Lipo, "Pulse Width Modulation for Power Converters - Principles and Practice," Wiley & IEEE Press, 2003.
- [45] S. K. T. Miller, T. Beechner, and J. Sun, "A comprehensive study of harmonic cancellation effects in interleaved three-phase VSCs," Proc. PESC'07, pp. 29-35, 2007.

- [46] W. R. Bennett, "New results in the calculation of modulation products," Bell Systems Technical Journal, 1933, vol. 12, pp. 228- 243.
- [47] A. K. Verma, B. Singh and D. T. Shahani, "Grid to vehicle and vehicle to grid energy transfer using single-phase bidirectional AC-DC converter and bidirectional DC-DC converter," International Conference on Energy, Automation and Signal, 2011, pp. 1-5, doi: 10.1109/ICEAS.2011.6147084.

APPENDICES

In this section, some applications of statistics are discussed which clarify statistics, especially probability distributions.

Appendix A: Bernoulli Distribution:

The Bernoulli Distribution is one of the simplest distributions since it has only two possible outcomes for a single trial. It is a building block for other more complicated discrete distributions. Any event where only two outcomes are possible with only one trial, this distribution can be used. For example, if a coin is tossed, the outcomes are either a head (H) or a tail (T). If we want to keep track of the head, then success is head, and the failure is a tail. When we toss a normal coin, the probability of a head or a tail is equal, that is $P(H) = 0.5$ and $P(T) = 0.5$. If we consider the probability of success to be 1 and the probability of failure to be 0, then $P(X=1) = 0.5$ and $P(X=0) = 0.5$, where X is the random variable.

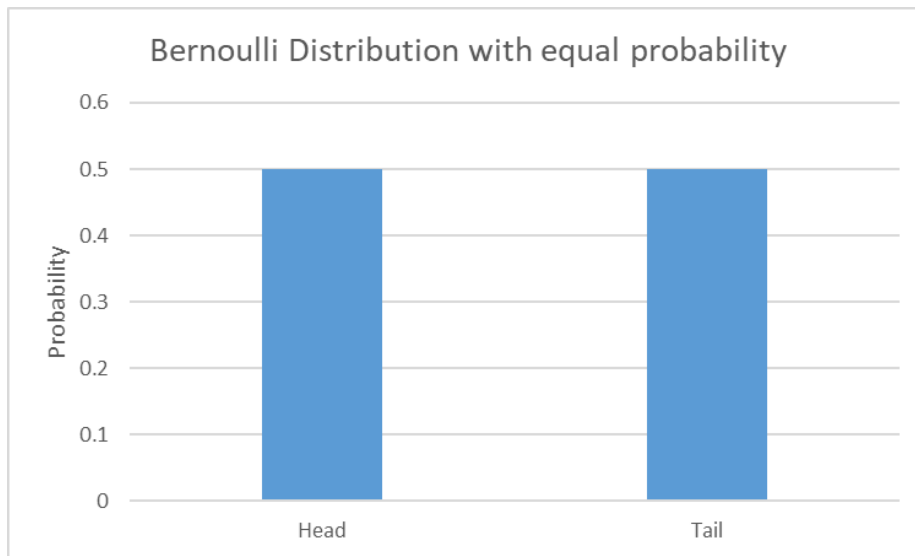


Figure A. 1: Bernoulli Distribution with equal probability

Similarly, if another coin is tossed, and the probability of a head or the probability of a tail are not equal, such as the probability of a head is 0.6, then the probability of a tail is, $P(T) = 1 - P(H)$ which is 0.4.

Conventionally the higher probability (success) is denoted with “p” and the lower probability (failure) with “1-p”. So, for the example above, probability of a head is p and the probability of a tail is (1-p). The graph in Figure A.2 shows the probability of a head and a tail for unequal probability.

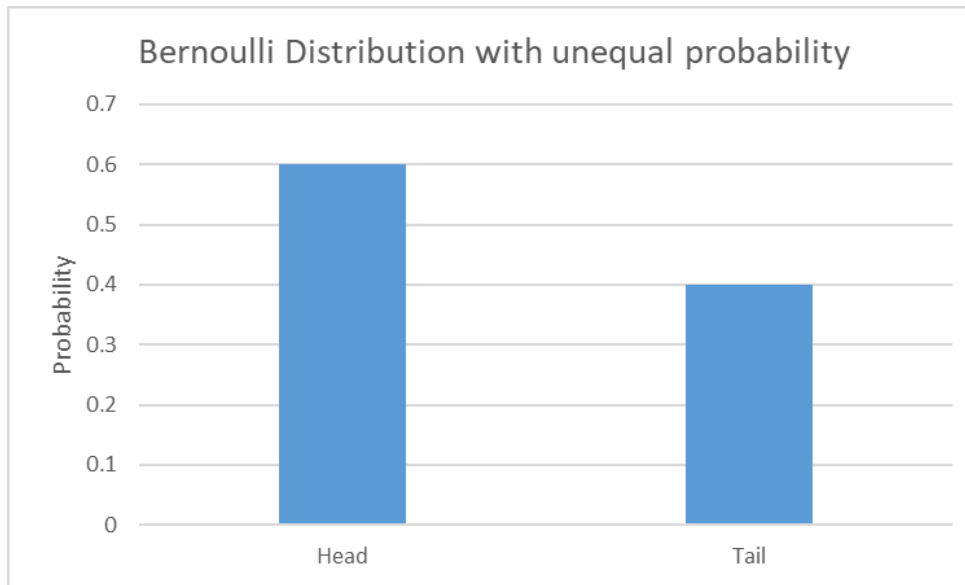


Figure A. 2: Bernoulli Distribution with unequal probability

Therefore, the expected value E of a random variable X from a Bernoulli Distribution can be written as:

$$E(X) = 1 \cdot p + 0 \cdot (1-p) = p$$

Since there is only one trial and a favored event, this outcome is expected to occur.

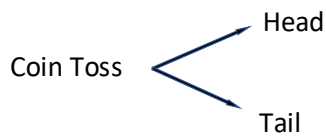
The Variance V of a random variable X from a Bernoulli Distribution is:

$$V(X) = E(X^2) - (E(X))^2 = p - p^2 = p(1-p).$$

Appendix B: Binomial Distribution:

As the name suggests, a Binomial Distribution has only two possible outcomes such as success/failure, gain/loss or win/lose. While a Bernoulli Distribution deals with the data which only has 1 trial and only 2 possible outcomes, a Binomial Distribution is the collection of Bernoulli trials for the same event. In other words, if a coin is tossed only once and the two outcomes—a head or a tail are observed, the random variable X follows a Bernoulli Distribution. However, if a coin is tossed multiple times and we observe the probability of obtaining heads k times, the random variable X follows a Binomial Distribution. Figure B.1 shows a difference between a Bernoulli Distribution and a Binomial Distribution.

Bernoulli Distribution



Binomial Distribution

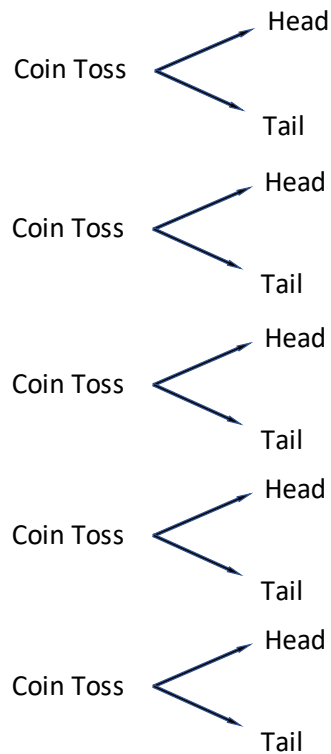


Figure B. 1: Bernoulli and Binomial Distributions

The Probability (P) can be calculated using the following Binomial Distribution formula:

$$P(x) = \frac{n!}{(n-x)!x!} p^x(1-p)^{n-x}$$

Where, n is the number of trials, x is the number of successful trials, p is the probability of success in a single trial. Some bar graphs showing the Binomial Distribution with different probabilities are shown in Figures B.2 and B.3. If a coin is flipped, the probability of it landing on its head side is equal to the probability of it landing on its tail side. In this case, the probability $p = 0.5$ or 50%. For example, if there are 20 trials, and the probability of success or failure is equal, x (number of success) is 50% of the number of trials (i.e., $x = 10$) as shown in Figure B.2. Similarly, if the probability of success is only 25%, then the x (number of success) is only a quarter of all trials i.e., only about 5 out of 20 trials as shown in Figure B.3a. Also, if the probability is high, for example 75%, the number of successes is about 15 out of 20 trials (Figure B.3b).

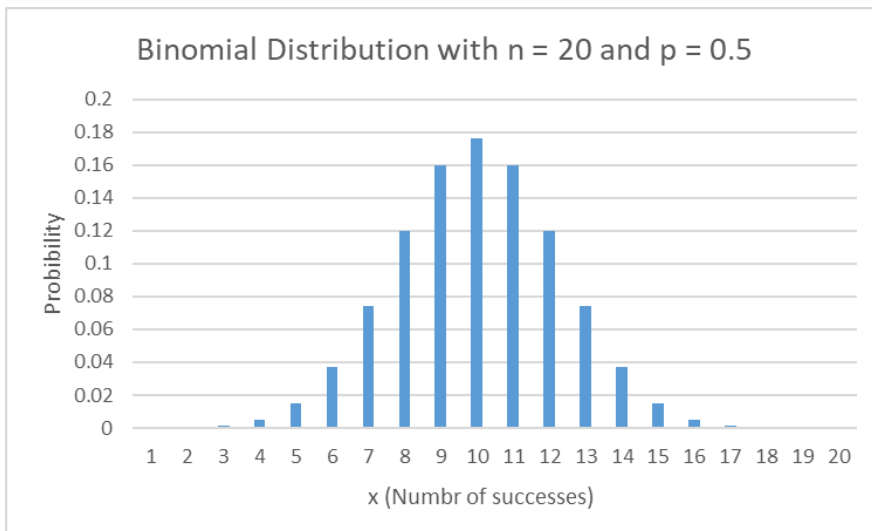


Figure B. 2: Binomial distribution when probability of success and failure are equal

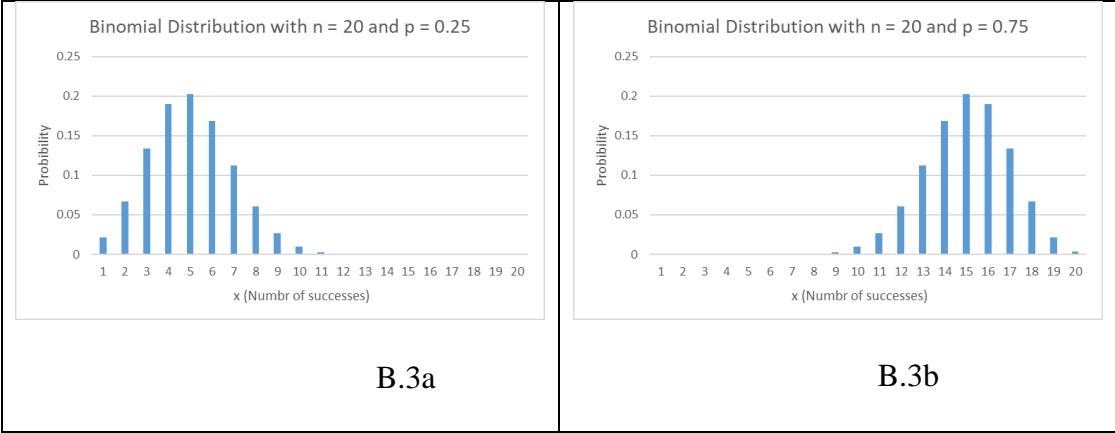


Figure B. 3: Binomial distribution when the probability of success and failure are not equal

Appendix C: Uniform Distribution:

Unlike a Bernoulli Distribution, all the possible outcomes of a uniform distribution are equally likely, such as rolling a fair dice. The probability density function of a random variable X is given by

$$P(X = x) = \frac{1}{b-a} \text{ for } -\infty < a \leq x \leq b < \infty$$

The Mean and the Variance of the discrete uniform distribution X on the interval $[a, b]$ are:

$$\text{Mean } E(X) = \frac{(a+b)}{2}$$

$$\text{Variance } V(X) = \frac{((b-a)+1)^2-1}{12}$$

For example, when rolling a 6-sided dice, the possible outcome values are 1, 2, 3, 4, 5, or 6 and each of the six numbers have an equal chance of appearing. Therefore, the Probability of each side is $P(X) = \frac{1}{6}$. The Expected value is $E(X) = \frac{6+1}{2} = 3.5$ and the Variance $V(X) =$

$$\frac{((6-1)+1)^2-1}{12} = \frac{35}{12} \approx 2.9167.$$

Appendix D: Normal Distribution:

The normal distribution, also known as the Gaussian Distribution, is one of the most important probability-distributions as it represents the behavior of most practical situations in the world. A normal distribution is perfectly symmetrical around its center and its Mean, Median and Mode values are all equal. The area under the normal distribution curve represents the probability and the total area under the curve sums to 1.

When both Mean and Variance are equal to 1, it is termed as “Standard Normal Distribution”. The normal distribution can be considered as the limiting case of a Binomial Distribution as the sample size becomes large in which case the Probability p becomes normal with Mean and Variance values.

The Probability Density Function of the normal distribution is given by:

$$f(x) = \left(\frac{1}{\sqrt{2\pi\sigma^2}}\right) \exp\left(-\frac{(x-\mu)^2}{2\sigma^2}\right) \quad -\infty < x < \infty$$

Where, $f(x)$ is the Probability Density Function, and the parameters μ is its Mean, and σ is its Variance. The Mean and Variance values characterize the graph of the normal distribution. The effects when Mean and Variance values vary are presented in Figures D.1-D.4 In Figures D.1 and D.2, the effects of change in the Mean value is studied by maintaining the same Variance and the effect of change in Variance is studied by maintaining the same Mean value in Figures D.3 and D.4. Most of the data values cluster around the average or Mean, and therefore when the value of the Mean increases from 3 to 18, the graph tends to shift to the right as seen in Figures D.1 and D.2. Similarly, when the Variance increases from 1 to 20, the graph tends to be flatter. Note that the colors used for the plots in Figure D.3 correspond with the colors used for the plots in Figure D.4

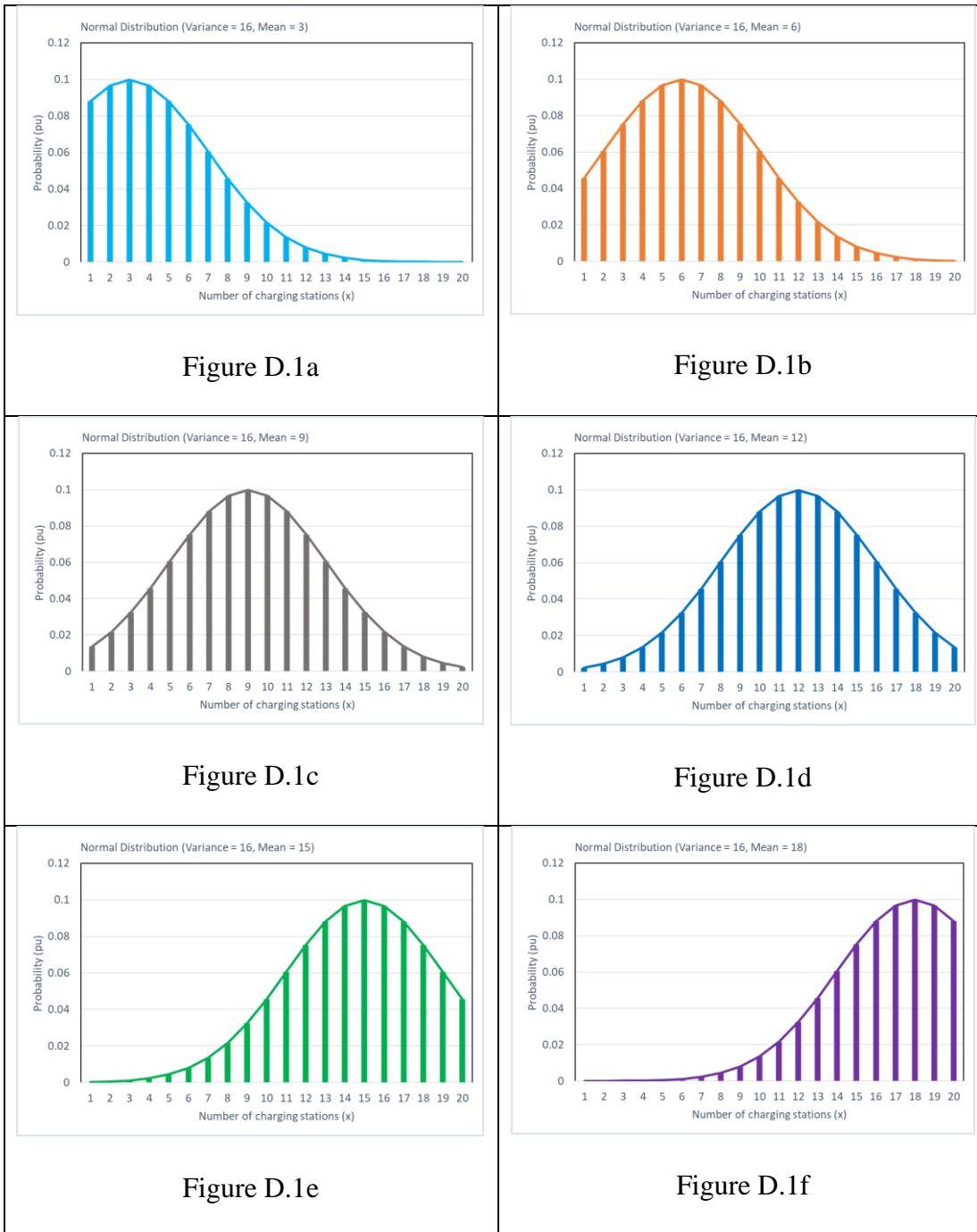


Figure D. 1: Normal distribution curves constant Variance and varying Mean

In Figure A.6a Mean is 3, in Figure A.6b Mean is 6, in Figure A.6c Mean is 9, in Figure A.6d Mean is 12, in Figure A.6e Mean is 15 and in Figure A.6f Mean is 18.

The shifts are visualized as shown in Figure D.7. The colors used for the plots in Figure D.6 correspond to the colors used in Figure D.7.

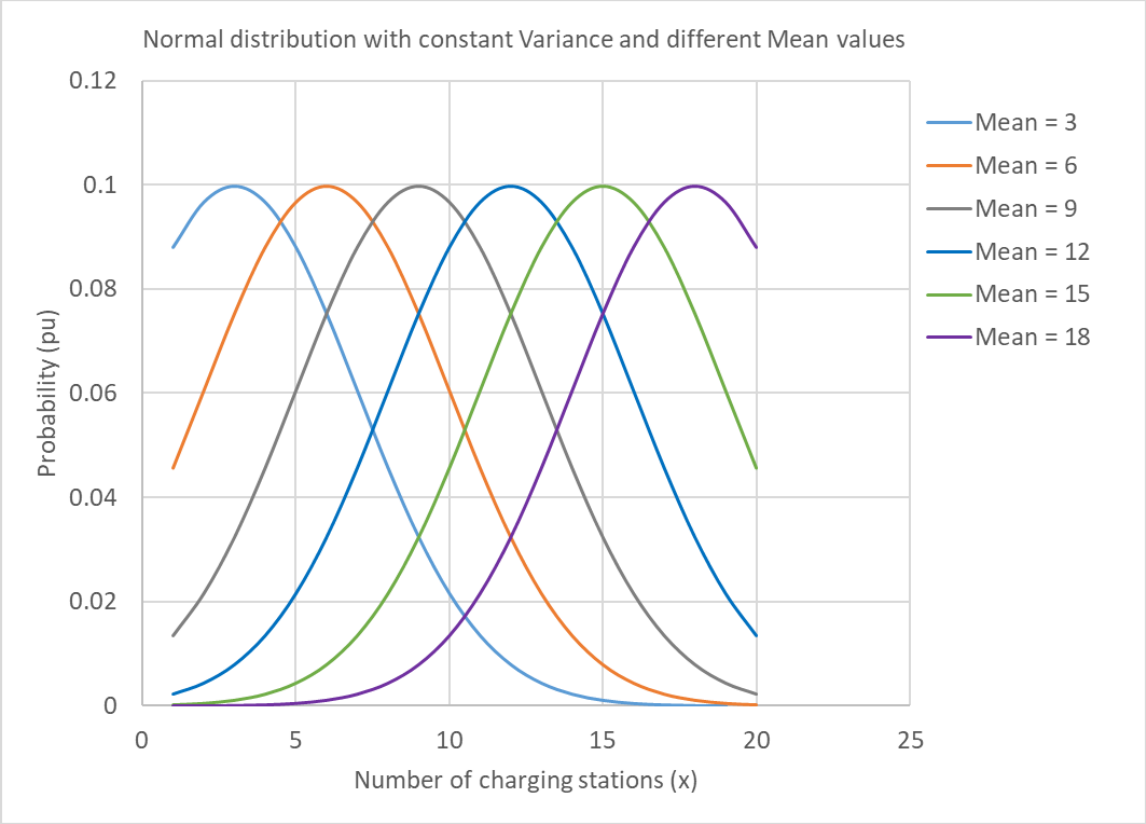


Figure D. 2: Graphs showing the shifting of the plots to the right as the Mean value increases



Figure D. 3: Normal distribution curves with constant Mean and varying Variance values

In Figure D.3a Variance is 1, in Figure D.3b Variance is 4, in Figure D.3c Variance is 9, in Figure D.3d Variance is 16 and in Figure D.3e Variance is 25.

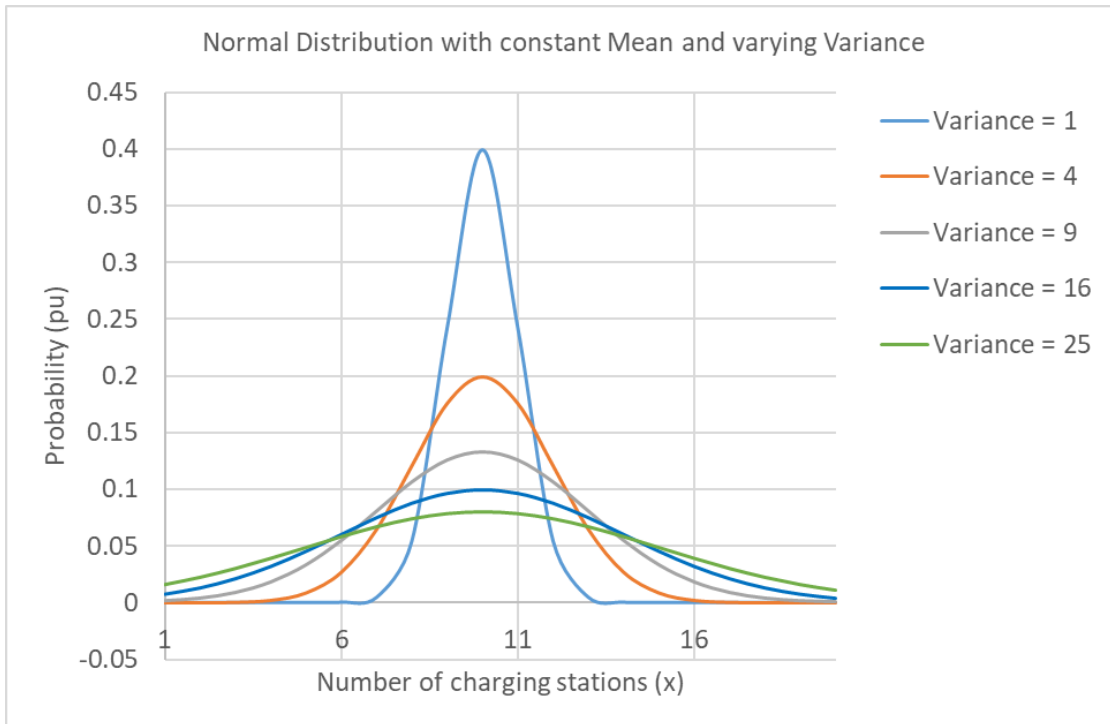


Figure D. 4: Graphs showing the steepness of the curves as the variance decreases

Appendix E: Poisson Distribution:

The Poisson Distribution is used to measure the probability of several events occurring within a given time interval, such as number of cars charging at a charging station during the day. The Poisson distribution is applicable in situations where the events occur completely at random in time or space. Successful events do not influence the probability that another successful event will occur.

The Probability Mass Function (PMF) of a Poisson random variable is given by:

$$P(X=x) = \frac{e^{-\lambda} \lambda^x}{x!} \quad \text{for } x = 0, 1, 2, \dots$$

where λ is the parameter of the distribution.

Like Binomial Distribution, the Poisson Distribution measures the number of when something happens, but unlike the Binomial, there is no specified number of n of possible tries. If an event happens independently and randomly over time, and the mean rate of occurrence is constant over time, then the number of occurrences in fixed amount of time will follow the Poisson Distribution. Figure E.1 shows the behavior of the Poisson Distribution for different mean values.

Similarly, the Inverse Poisson Distribution is used to find the Average number λ if the probability is known, for a fixed interval of time.

Like Poisson Distribution, if the average rate at which the events occur is known for a fixed time interval, the Cumulative Poisson Distribution helps to predict the probability that an event occurs less than or equal to x times within that interval.

For example, if on average 5 cars charge at a charging station in 2 hours (say, between 9 am and 11 am), what is the probability that 0 to 3 cars (less than or equal to 3 cars) charge during the same period, the next day?

Here, we calculate the probabilities of 0 car charging, 1 car charging, 2 cars charging, and 3 cars charging and sum (accumulate) them all to get the Cumulative Poisson Distribution, i.e.,

$$P(X=0) = \frac{e^{-5}5^0}{0!} = 0.0067$$

$$P(X=1) = \frac{e^{-5}5^1}{1!} = 0.0336$$

$$P(X=2) = \frac{e^{-5}5^2}{2!} = 0.0842$$

$$P(X=3) = \frac{e^{-5}5^3}{3!} = 0.1403$$

Therefore, $P(X \leq 3) = 0.0067 + 0.0336 + 0.0842 + 0.1403 = 0.26$ or 26%

So, the probability that less than or equal to 3 cars charging within the next day is 26%.

To compare Normal Distribution versus Poisson Distribution, it is noted that while Normal Distribution is continuous, Poisson Distribution is discrete. Also, Normal Distribution describes continuous data which have a symmetric distribution, and thus will have a ‘bell’ shape whereas, Poisson Distribution is not symmetric. In a Normal Distribution, the Mean and the Variance values are different, but in the Poisson Distribution Mean and Variance values are the same. The following derivation shows that both Mean and Variance values of the Poisson Distribution are the same:

$$P(X=x) = \frac{e^{-\lambda}\lambda^x}{x!}$$

$$\text{Mean } E(x) = \sum_{x=0}^{\infty} x P(x) = \sum_{x=0}^{\infty} x \frac{e^{-\lambda} \lambda^x}{x!} = 0 \frac{e^{-\lambda} \lambda^0}{0!} + 1 \frac{e^{-\lambda} \lambda^1}{1!} + 2 \frac{e^{-\lambda} \lambda^2}{2!} + 3 \frac{e^{-\lambda} \lambda^3}{3!} + \dots =$$

$$0 + e^{-\lambda} \lambda + e^{-\lambda} \lambda^2 + \dots$$

$$= e^{-\lambda} \lambda (e^{\lambda}) = \lambda$$

Therefore, Mean $E(x) = \lambda$

Now let's find the Variance:

$$\text{Variance } \sigma^2 = E(x^2) - [E(x)]^2$$

$$E(x^2) = \sum_{x=0}^{\infty} x^2 P(x) = \sum_{x=0}^{\infty} x + x(x-1)P(x) = \sum_{x=0}^{\infty} x + x(x-1) \frac{e^{-\lambda} \lambda^x}{x!}$$

$$= \sum_{x=0}^{\infty} x + x(x-1) \frac{e^{-\lambda} \lambda^x}{x!} = \sum_{x=0}^{\infty} x \frac{e^{-\lambda} \lambda^x}{x!} + \sum_{x=0}^{\infty} x(x-1) \frac{e^{-\lambda} \lambda^x}{x!}$$

$$= \lambda + 0 + 0 + \frac{2e^{-\lambda} \lambda^2}{2!} + \frac{6e^{-\lambda} \lambda^3}{3!} + \dots = \lambda + e^{-\lambda} \lambda^2 (1 + \frac{\lambda}{1} + \frac{\lambda}{2} + \frac{\lambda}{3}) = \lambda + e^{-\lambda} \lambda^2 e^{\lambda} = \lambda + \lambda^2$$

$$\text{Therefore, } E(x^2) = \lambda + \lambda^2$$

$$E(x^2) - [E(x)]^2 = \lambda + \lambda^2 - \lambda^2 = \lambda$$

$$\text{Therefore, Variance } \sigma^2 = \lambda$$

Hence, both Mean and Variance values are the same in Poisson Distribution.

Figures E.1 and E.2 show the effect of change in Mean values to the Poisson Distribution and Cumulative Poisson Distribution respectively. As can be seen in both the figures, as the Mean value changes, most of the data shifts and tends to cluster around the Mean. When the Mean increases from 3 to 18, the center of the graph shifts to the right.

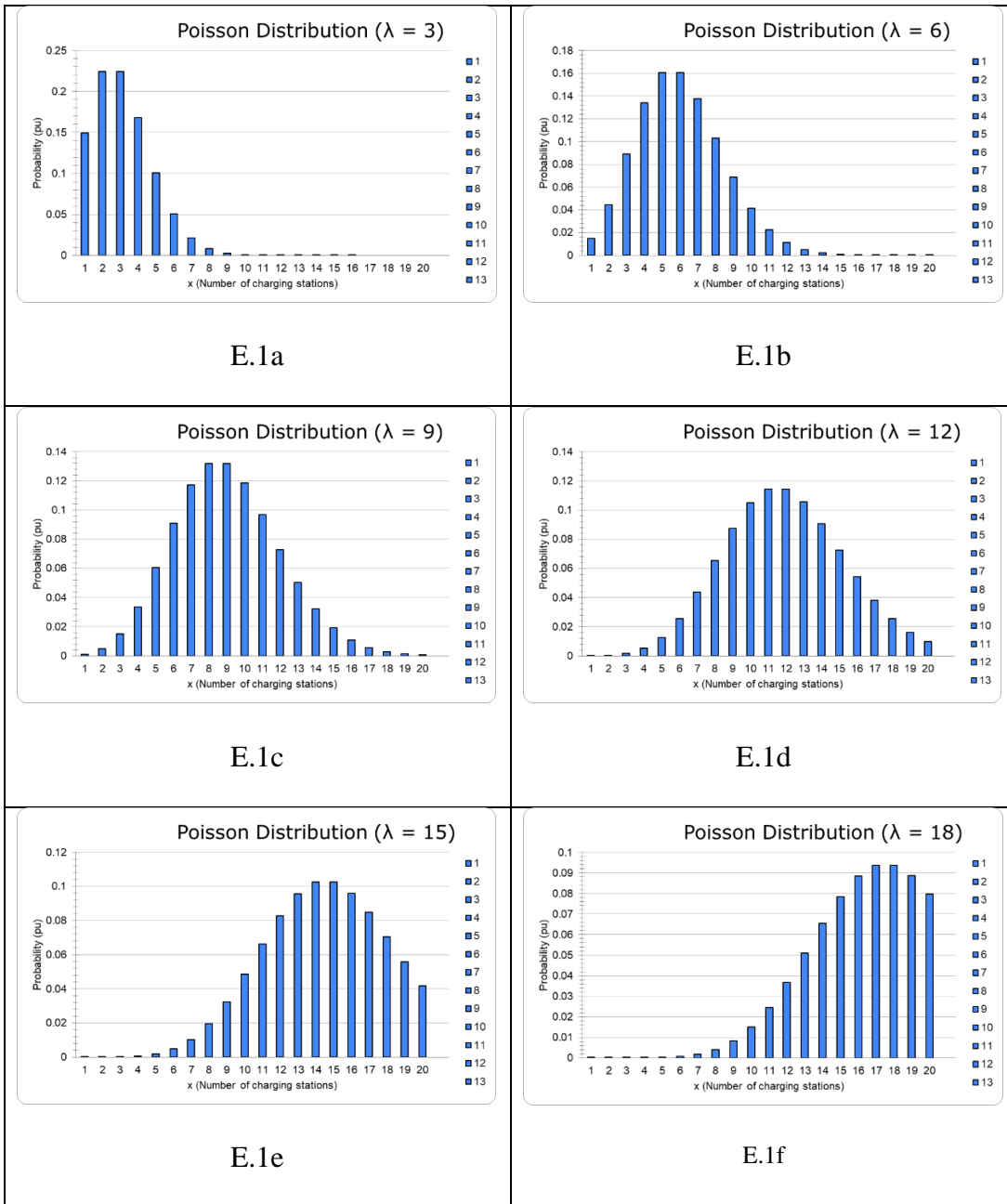


Figure E. 1: Bar graphs showing the behavior of the Poisson Distribution as the Mean value varies

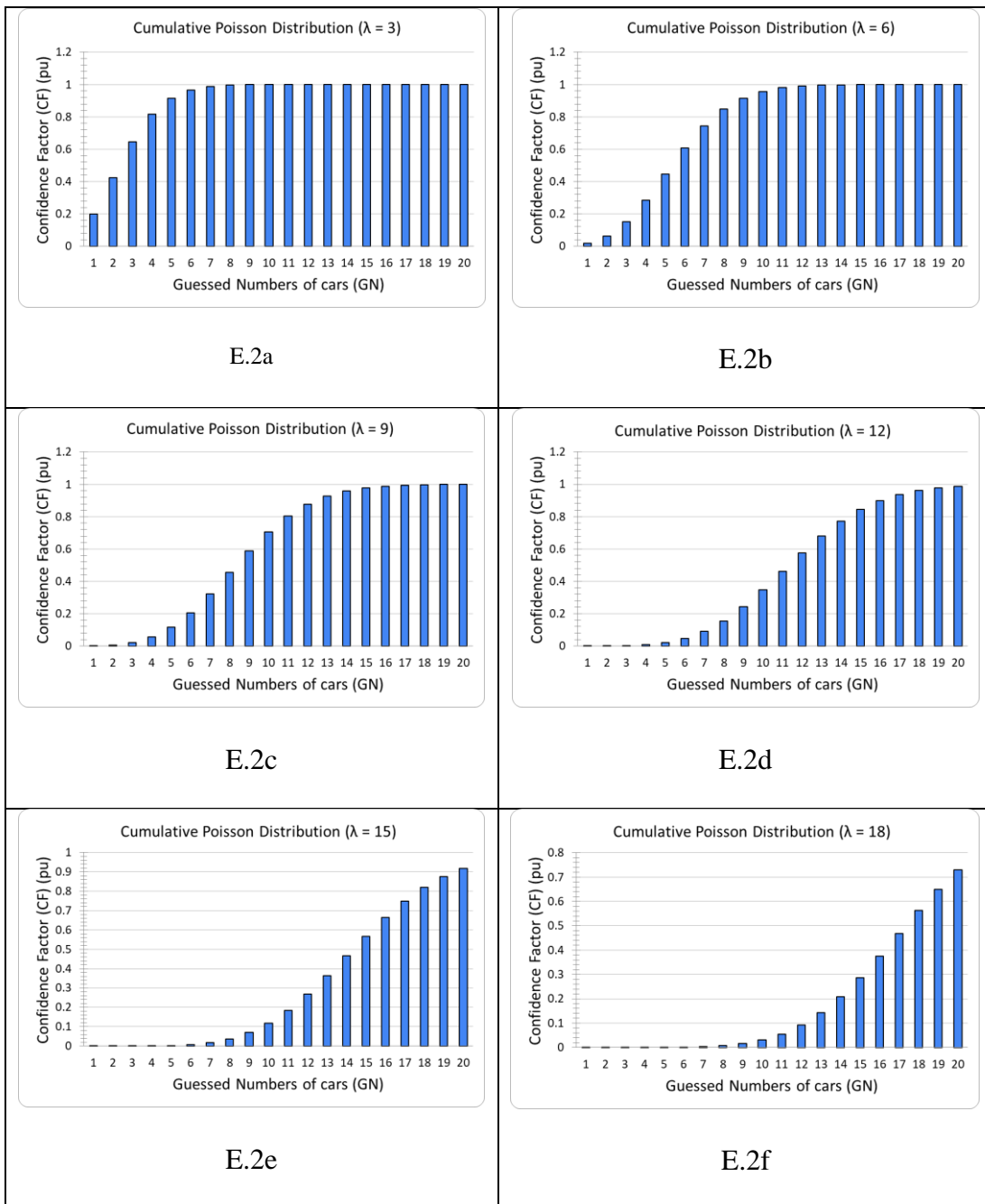


Figure E. 2: Behavior of the Cumulative Poisson Distribution as the Mean value varies

